Planetary and Space Science 119 (2015) 137–154

Contents lists available at ScienceDirect

Planetary and Space Science

journal homepage: www.elsevier.com/locate/pss

Inferring alteration conditions on Mars: Insights from near-infrared spectra of terrestrial basalts altered in cold and hot arid environments

Joanna Gurgurewicz [a,b,*], Daniel Mège [b,c,d], Véronique Carrère [c,d], Anne Gaudin [c,d], Joanna Kostylew [e], Yann Morizet [c,d], Peter G. Purcell [f], Laetitia Le Deit [c,d]

[a] Institute of Geological Sciences, Polish Academy of Sciences, Research Centre in Wrocław, Podwale St. 75, PL-50449 Wrocław, Poland
[b] Space Research Centre, Polish Academy of Sciences, Bartycka St. 18A, PL-00716 Warsaw, Poland
[c] Laboratoire de Planétologie et Géodynamique, UMR CNRS 6112, Université de Nantes, 2 rue de la Houssiniere, 44322 Nantes, France
[d] Observatoire des Sciences de l'Univers Nantes Atlantique, UMS CNRS 3281, 2 rue de la Houssiniere, 44322 Nantes, France
[e] Institute of Geological Sciences, University of Wrocław, Cybulskiego St. 30, PL-50205 Wrocław, Poland
[f] P&R Geological Consultants, 141 Hastings Street, Scarborough, WA 6019, Australia

ARTICLE INFO

Article history:
Received 15 January 2015
Received in revised form
10 July 2015
Accepted 2 September 2015
Available online 18 September 2015

Keywords:
Basalt alteration
Near-infrared spectroscopy
Terrestrial analogs
Mars

ABSTRACT

Can information on the Martian environmental conditions prevailing during the alteration of its basaltic crust be inferred from near-infrared (NIR) spectra? In order to determine whether basalts altered under arid conditions but different temperatures have different spectral signatures, NIR spectra of basalts altered in cold (Udokan volcanic field, Siberia) and hot (Ogaden Basin, Ethiopia) environments were obtained. The NIR spectra of the alteration rind surface and the internal part of the studied samples are similar, suggesting that the NIR spectra of Martian bulk rocks may be of limited help in identifying paleoenvironment conditions. Bulk rock spectra analysis reveals, however, that spectra of the least altered rocks display clear absorption bands of smectites, suggesting that a distinction between clay minerals in weakly weathered basalts and clay-rich formations cannot be based solely on analysis of infrared spectra obtained from orbit. Additional compositional information can be retrieved from rock powder spectra – zeolites present in the Udokan basalt spectra might be used to infer composition and temperature of the fluids from which they precipitated. The presence of calcite and iddingsite is ascertained by other methods, but they are not apparent in bulk rock spectra and only weakly apparent in powder spectra. The basalt samples studied display alteration products that reflect their different alteration histories; nevertheless no criterion has been found that would help in identifying the origin of the weathering water – subsurface, rainfall, or snowfall.

1. Introduction

Mafic rocks are widespread at the surface of Mars. Their existence has been inferred from the composition of Martian meteorites (Nyquist et al., 2001), from geomorphology, even outside the large volcanoes (e.g., Mège and Masson, 1996; McEwen et al., 1999; Mège et al., 2003), and also from several orbital infrared data sets: TES onboard Mars Global Surveyor (Christensen et al., 2000; Hamilton et al., 2001; Wyatt and McSween, 2002; Christensen et al., 2005; Rogers and Christensen, 2007; Rogers et al., 2007; Edwards et al., 2008; Koeppen and Hamilton, 2008), OMEGA onboard Mars Express (Mustard et al., 2005; Kanner et al., 2007), and CRISM onboard Mars Reconnaissance Orbiter (Salvatore et al., 2010). Evidence of basaltic surface composition comes from characteristic absorption bands of olivine and pyroxene, and mineralogical abundance modeling (Wyatt et al., 2001; Poulet et al., 2009). Based on analyses of TES data, Wyatt and McSween (2002) suggested that the basalts in the southern hemisphere are mainly fresh, while the surface of the northern hemisphere is composed of weathered basalt, which has been previously interpreted by Bandfield et al. (2000) as a basaltic andesite. The TES results have been confirmed and refined by analysis of OMEGA and CRISM datasets (Bibring et al., 2005, 2006; Mustard et al., 2005, 2008; Poulet et al., 2007, 2009). In addition to orbital data, *in situ* spectra obtained from Pancam (Bell et al., 2004), Mössbauer spectrometer (Morris et al., 2004), mini-TES and APX Spectrometer (McSween et al., 2004) unambiguously demonstrated the presence

* Corresponding author at: Institute of Geological Sciences, Polish Academy of Sciences, Research Centre in Wrocław, Podwale St. 75, PL-50449 Wrocław, Poland. Tel.: +48 713376344.
E-mail address: jgur@cbk.waw.pl (J. Gurgurewicz).

http://dx.doi.org/10.1016/j.pss.2015.09.002
0032-0633/

of basalts at the Spirit rover landing site in Gusev crater. Mini-TES data have been used by Rogers and Aharonson (2008) to determine the mineral composition of the basaltic soils at the Meridiani Planum – Opportunity rover landing site. Basaltic rocks have also been found at the Pathfinder landing site by the Pathfinder IMP imager (Bell et al., 2002), despite the different environmental settings – the Ares Vallis floodplain.

Of interest is whether information on the climate conditions prevailing during basalt alteration can be inferred from near-infrared spectra. Determining terrestrial paleoclimate conditions using secondary mineral assemblages has been the subject of many studies, but remains quite a challenge because these assemblages depend not only on climate, but also on climate history, lithology, rock fracturing, groundwater circulation, diurnal temperature variations, and morphology (Bender Koch et al., 1995; Vogt and Larqué, 2002; Deepthy and Balakrishnan, 2005; Vogt et al., 2010). In this paper, we investigate the record of climatic conditions in near-infrared (NIR) spectra of basalt samples from arid cold and arid hot environments, as well as hot environments in which wet and arid climates occurred successively. Any of these conditions may have been representative of the alteration conditions on Mars. Indeed, it has been argued that the present cold and arid alteration conditions at the surface of Mars (e.g., Bishop et al., 2002; Levrard et al., 2004), though probably dominant throughout the Martian history (Carr and Head, 2010), may have been interrupted by episodes of warmer and/or wetter conditions (McKeown et al., 2009; Gaudin et al., 2011; Le Deit et al., 2012).

Secondary mineral assemblages observed in the spectra may reflect variations in alteration conditions. In addition to temperature and humidity, the pH conditions during alteration play an important role in the formation of the secondary minerals. Acidic conditions of basalt alteration prevailed in the early Martian history (e.g., Bibring et al., 2006), justifying that some works have focused on the products of basalt alteration on Mars from study of terrestrial analogs in acidic environment (e.g., Hynek et al., 2013). This study concerns the terrestrial basalts altered in conditions of moderate pH and potentially comparable to environmental conditions during other Martian periods. The studied basalts are located in the Udokan area of Siberia, and in the Ogaden region of southeast Ethiopia (Fig. 1, Table 1).

2. Geology and climate context of the studied basalts

The mid-Miocene to Quaternary Udokan volcanic field is a part of the 1500 m-high Udokan range located in the northeastern part of the Baikal Rift Zone (Rasskazov, 1994; Petit and Déverchère, 2006). It is correlated with the northeastern most thermal anomaly associated with the rift (Lysak, 1995). The samples studied are from a lava flow (Fig. 2a and b) from a Pleistocene volcanic cone (Stupak et al., 2008). At that time, the climate in the Baikal area was undergoing "cryo-aridization" (Sheinkman, 2003), changing from cool continental to arctic (Shchetnikov et al., 2012), subsequent to which oscillations between cold and arctic conditions have occurred (Demske et al., 2005; Enikeev, 2008; Tarasov et al., 2009). In the present conditions, the basalts are being altered under a cold and dry climate (climate zone *Dwc*, according to the Köppen–Geiger classification (Peel et al., 2007)) having long cold winters (average temperatures ranging from −24 to −37 °C during 6 months at the Naminga meteorological station located 30 km away from the sampling sites (Table 1), at a similar elevation 1440 m a.s.l., with absolute minimum of about −60 °C) and short warm summers (10–15 °C during 3 months). Precipitation is 740 mm/year, including 1/3 as snow (Afonin et al., 2008; SRK Consulting, 2010). The alteration rinds of the studied basalt samples are markedly dissimilar: from pellicular to thick (3 mm) with a diffuse or sharp contact with the internal part of the rock.

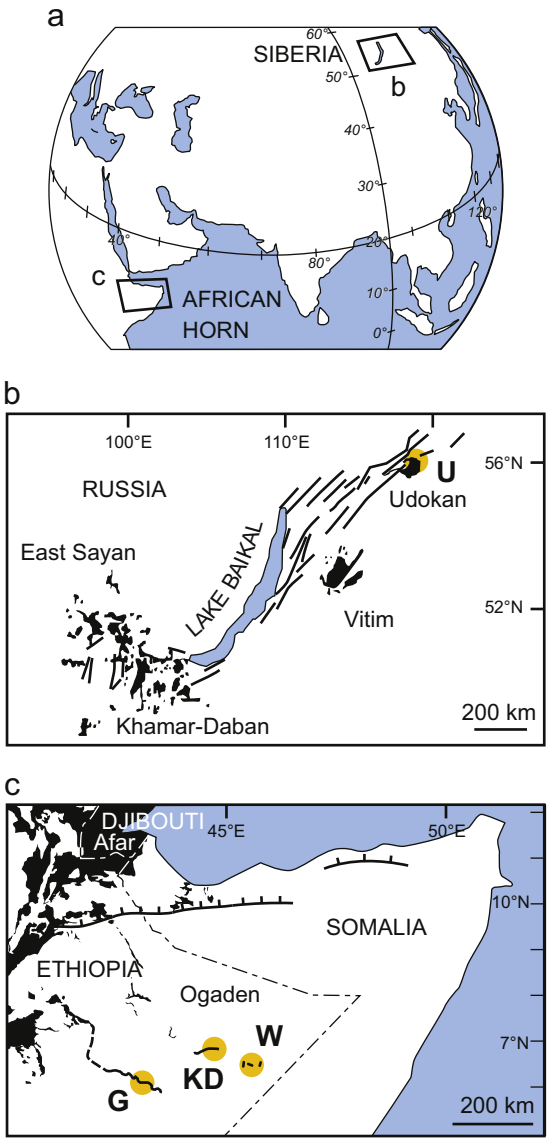

Fig. 1. Location of the Cenozoic Udokan volcanic field and Ogaden basalts. The dark patches are the volcanic exposures. The sampling sites are shown by circles: U – Udokan volcanic field; G – north of Gode town; KD – east of Kebri Dehar town; W – south of the Werder town.

Table 1
Location of the analyzed samples from the Udokan and Ogaden regions.

Sample	*Region*	*Site*	*Latitude*	*Longitude*	*Elevation a.s.l. (m)*
RN01A/B	Udokan	1	56°24′55″N	118°9′28″E	1629
RN02	Udokan	2	56°24′44″N	118°9′31″E	1644
RN03	Udokan	3	56°24′31″N	118°9′1″E	1498
RN04	Udokan	4	56°24′31″N	118°9′1″E	1498
K1.30	Ogaden	Kebri Dehar	6°45′18″N	44°26′3″E	538
K3.1	Ogaden	Kebri Dehar	6°49′38″N	44°65′50″E	627
W1.4	Ogaden	Werder	6°23′58″N	45°49′19″E	485
W2.5	Ogaden	Werder	6°24′35″N	45°38′3″E	508
W3.2	Ogaden	Werder	6°23′4″N	45°30′13″E	524
WS1.2	Ogaden	Gode	6°1′11″N	43°21′56″E	314

The Ogaden Basin in southeastern Ethiopia displays lava flows of Oligocene to Neogene age (Mège et al., 2015a) that were extruded following uplift of the region between the Cretaceous and Paleocene (Bosellini, 1989). Since the Oligocene, the regional

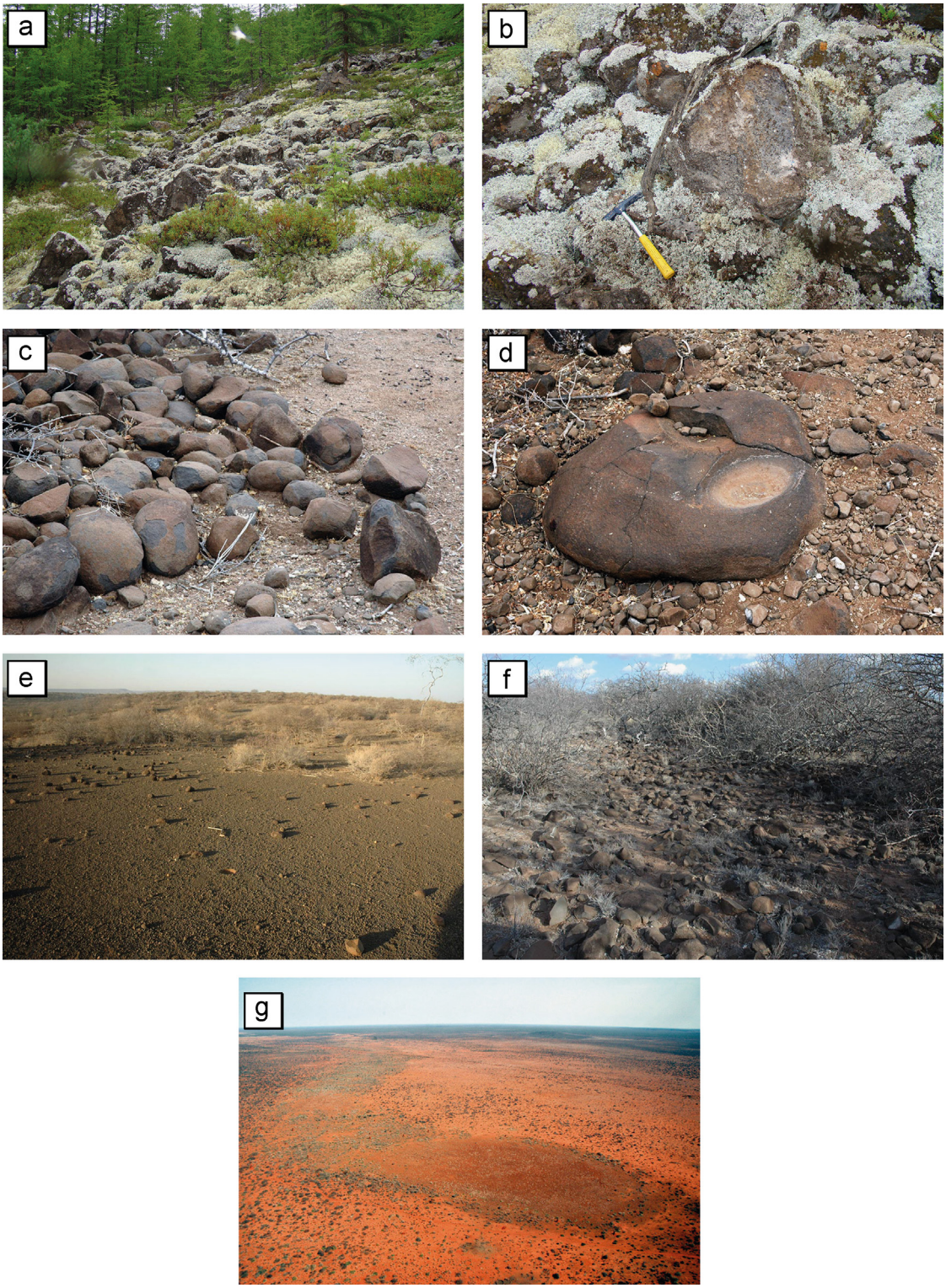

Fig. 2. Field views of the sampling sites: (a, b) Udokan volcanic field, Baikal Rift Zone, Siberia. Basalts are extensively coated by lithobionts; (c) Ogaden, Kebri Dehar: spheroidal weathering of basalt with onion-like layers; (d) Ogaden, Kebri Dehar: intense rainfall (usually a few times a year) contributes to rock alteration in addition to diurnal moisture contrasts. After rainfall, water may stagnate on basalt surface cavities, increases weathering within the cavities, and evaporates (note the concentric salt deposits in the hollow). Next rainfall washes the rock and removes the clay particles from its surface, which enlarges the surface cavities. Basalt-derived clays accumulate in pans; (e) Ogaden, Werder area; (f) Ogaden, Gode area; (g) Ogaden, Werder: accumulation of basalt-derived clays in a pan. The channel that transports clays from the basalt exposure to the pan is visible on the left side of the image.

uplift is a consequence of vertical plate motions accompanying the development of the Main Ethiopian Rift to the west and the Afar Depression to the north (Mège et al., 2015a). Three sampling sites have been studied: Gode, Kebri Dehar, and Werder (Table 1, Figs. 1 and 2c–f). Hard rock outcrops are infrequent; the basalt exposures are usually cobbles and pebbles on coarse grit mounds or small hills ranging in height to about 40 m above local average. The sampled basalts are all untransported cobbles located on such hills

(Mège et al., 2008); they are not part of a pedogenetic profile. During torrential rains, the alteration products are removed from the surface of the cobbles (with the exception of some surface irregularities, Fig. 2d), and accumulate downslope in ponds that subsequently dry out into hard semi-circular pans (Fig. 2g).

The Gode basalts are part of a large 'meandering' landform caused by exhumation of a river channel-filling basalt flow. Its $^{40}Ar/^{39}Ar$ age is $\sim 7.46 \pm 0.47$ Ma (Mège et al., 2015b). The sampling site, at the top of the flow, is estimated to be 600+ km away from the erupting vent (Mège et al., 2015a). The Kebri Dehar basaltic flow also followed a river channel but is dated at 27.6 ± 0.5 Ma ago from two $^{40}Ar/^{39}Ar$ ages (77% plateau age and 79% inverse isochron age). The Werder basalts are fissure flows located close to the lava eruption site (Mège and Purcell, 2010). They have been dated as 29.9 ± 1.9 Ma (83% plateau age) to 25.4 ± 0.7 Ma (74% inverse isochron age). The present alteration conditions are hot and arid (climate zone *Bwh* in the Köppen–Geiger classification (Peel et al., 2007)), with a mean temperature of 27–30 °C. Mean rainfall is < 200 mm/year, and is zero or almost zero over at least nine months a year (Kohler and Krauer, 1996; NOAA, 2012). Rain does not fall every year. Alteration is thought to be facilitated in large degree by the wetting effects of common early morning dew. The alteration conditions for the Gode basalts probably has not changed appreciably since their eruption because of globally high and increasing aridity, nuanced at the second order by climate oscillations (deMenocal, 1995; Feakins et al., 2005; Huang et al., 2007; Bonnefille, 2010) driven by ice-sheet growth and retreat events (Clark et al., 1999). The alteration rind is pellicular.

The alteration conditions of the Kebri Dehar and Werder basalts since their emplacement during Late Oligocene are less constrained by the existing paleoclimate data. Although there is little doubt that temperatures that existed since the Oligocene were high, as shown by carbonate platforms adjoining the fully emerged Ogaden and western Somalia (Bosellini, 1989), humidity indicators are scarce. Especially, the well-known Chilga fossil locality (Upper Oligocene), where seasonal precipitation and groundwater table fluctuations are well documented (Jacobs et al., 2005), is in the middle of the developing Ethiopian flood-basalt province, whereas the Ogaden is only on the outskirts (Mège et al., 2015a; Mège and Korme, 2004). After the globally wet Eocene climate optimum, the general trend has been toward increased aridity but with complex modulations (Bobe, 2006; Feakins, 2013) related to the development of the Sahara desert (Micheels et al., 2009), the development of the East African Rift topography (Sepulchre et al., 2006), and the Messinian salinity crisis in the Mediterranean region (Feakins, 2013). Paleobotanic sampling indicates gradual extension of grass-dominated savanna in eastern Africa between middle and upper Miocene (Jacobs, 2004; Pound et al., 2012), concomitant with a general drying trend (Huang et al., 2007) indicated by the changing paleoenvironments associated with rodents in Kenya (Winkler, 2002). The alteration rind of the Werder basalt sample is thicker (5 mm) than the alteration rind of the Gode basalt sample and its transition to the fresh rock is diffuse, whereas the Kebri Dehar basalt sample shows a rind of intermediate thickness (2 mm) but in sharp contact with the internal, fresher rock.

The three Ogaden sites – Gode, Kebri Dehar and Werder – are, therefore, representative of three slightly different alteration environments (Table 2). The Gode basalts are representative of the present hot and arid conditions. Although emplacement in a river channel indicates that part of the flow may have been initially in

Table 2
Alteration conditions at the sampling sites.

Site	*Alteration conditions and history*
Udokan	Cold and arid, no groundwater (present-day conditions)
Gode (Ogaden)	Hot and very arid, no groundwater (present-day conditions)
Kebri Dehar (Ogaden)	Hot with globally increasing aridity since Late Oligocene; possible alteration by groundwater in the past
Werder (Ogaden)	Hot with globally increasing aridity since Late Oligocene; no groundwater

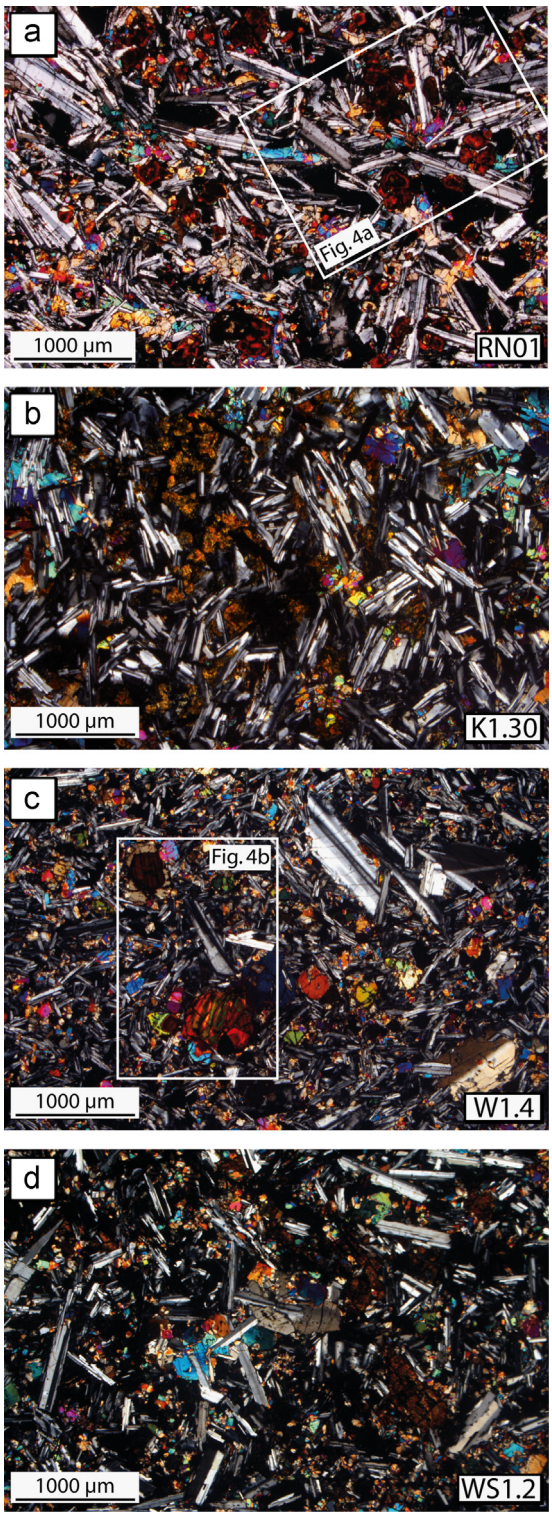

Fig. 3. Photomicrographs of the representative basalts samples from Udokan (Siberia) and Ogaden (Ethiopia): (a) Udokan, site 1; (b) Ogaden, Kebri Dehar; (c) Ogaden, Werder; (d) Ogaden, Gode. Polarizing microscope, crossed polars.

contact with groundwater, the very thin alteration rind argues against significant influence of groundwater on alteration. The Kebri Dehar basalts have a thicker alteration rind and have undergone a longer alteration history, including periods of wetter conditions and, perhaps, alteration by groundwater. The Werder basalts also have a thick alteration rind and underwent the same succession of environments as the Kebri Dehar basalts. However, their fissural emplacement and the local geology (Mège et al., 2008) indicates that they were part of a volcanic edifice above any regional water table. It is inferred that the Werder basalts were altered by rainfall water and perhaps, hydrothermal fluids during emplacement.

3. Samples and methods

The basalt samples from Udokan (Fig. 2a, b) and Ogaden (c–g) were collected in the field in 2008 and included basaltic rocks at various stages of alteration. Two Udokan samples were extracted from the upper surface of a continuous lava flow exposure, and the others and the Ogaden samples are cobbles formed by widening of joints at the surface of the lava flow. Twenty-four samples have been studied (five from Udokan and nineteen from Ogaden): all are alkali basalts, Ti-rich, with a slightly higher Ti content in the Udokan samples (Gurgurewicz, 2010). Although the Martian samples studied *in situ* are tholeiitic (McSween et al., 2004), the variety of lava flow morphologies and diversity of volcanic edifices observed on the whole Martian surface suggest also that the actual difference in viscosity, and therefore composition of the lavas, is huge.

The Udokan basalts are vesicular. The mineralogical structure of the Udokan and Ogaden basalts is similar (Fig. 3a–d). Plagioclase, pyroxene and olivine are the main components of the groundmass, which also contains opaque minerals, rhönite (Ogaden basalts), and occasionally glass. The phenocrysts include mainly plagioclase and iddingsitized olivine (Fig. 4).

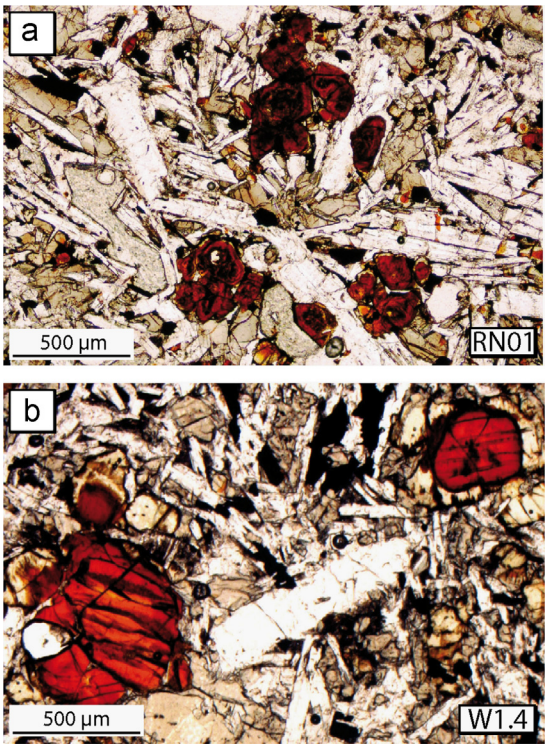

Fig. 4. Photomicrographs of the iddingsitized olivine in the Udokan (a) and Ogaden (b) basalt samples. Polarizing microscope, plane polarized light.

Reflectance has been measured using the ASD FieldSpec® 3 spectrometer in the spectral range of 0.35–2.5 μm, with 3 nm spectral resolution in the visible range and 10 nm in the infrared. Ninety-one spectra were acquired, both of the alteration rind surface and the internal part of the bulk samples, and of the whole-rock powders. A Spectralon™ surface was used as the reflectance standard. For the bulk samples, the Hi-Brite contact probe was placed perpendicular to, and against the fractured sample. The powders were obtained by crushing the rocks manually using an Abiche mortar to a grain size <2 mm, then powdering them finely in an agate grinder. The obtained powders were then dry sieved to a grain size <25 μm. During measurement, the contact probe was placed a few millimeters above, and perpendicular to the flattened powder surface. Care was taken not to compress the powder during flattening. Ten spectra were averaged for each sample spot of diameter 10 mm. The scatter between the ten spectra, calculated as the standard deviation of the reflectance divided by the square root of the number of spectra, was very low, on the order of 10^{-5}–10^{-4}. The offsets in the spectra at 1.0 and 1.8 μm have been corrected by splice correction using ViewSpec™ Pro. Absorption features observed in spectra obtained with the ASD spectrometer have been used to determine the mineral content and hydration. However, whereas the ASD can detect Fe-bearing silicates, it cannot reliably detect plagioclases, which are one of the major components of the analyzed basalt samples, but their characteristic absorption bands are at longer wavelength. The spectra that were used to identify minerals have been selected from various libraries (see the figure annotations), with a preference toward samples for which accurate contextual descriptions are available.

In order to retrieve more detailed information on groundmass mineral composition, the samples from the Udokan volcanic field and samples representative of each Ogaden sampling site have been analyzed using X-ray diffractometer Siemens D5005 or D5000. The powder mounts of the whole-rock samples were scanned at 30 kV and 20 mA, from 2° to 65°θ using Cu-Kα radiation (Ogaden) or from 4° to 75°θ using Co-Kα radiation (Udokan) at a speed of 1.2°θ/min. The presence of a broad peak in the diffractograms at $2\theta=6°$ was the selection criterion for extraction of the clay-sized fraction. For identification of the major clay types, the <2 μm clay-sized fractions were extracted by sedimentation in distilled water. The wet fractions were smeared on glass slides to make the specimens which after air-drying were X-rayed from 2° to 25°θ. Selected specimens that contained an adequate amount of clay were X-rayed again after glycol treatment, to estimate the difference in clay content. The background of the patterns was subtracted from peaks using the EVA© software. Mineral phases were then identified and the intensity of diffraction peaks retrieved using the EVA© software and the PDF 2 database provided by the International Centre for Diffraction Data (ICDD).

Compositional analyses using micro-Raman spectrometer have been carried out for complementing data obtained using other instruments. The Raman scattering was excited using an Innova 300-5 W Argon ion laser from Coherent© operating at 514 nm in wavelength and the spectra were collected using a Jobin-Yvon LabRam® spectrometer (focal distance = 300 mm) equipped with a 2400 grooves/mm CCD detector. The analyses were performed in confocal mode (hole = 500 μm, slit = 200 μm). We performed the analyses using a x50 Olympus objective reducing the analyzed sample volume size (few μm^3). The spectral frequency position was calibrated using the emission lines of Ne- and Hg-lamps with an accuracy within ± 1 cm^{-1}. The spectra were acquired at room temperature and no correction was applied for the dependence of the scattered intensity on temperature and frequency (Neuville and Mysen, 1996; Long, 2002; Morizet et al., 2010).

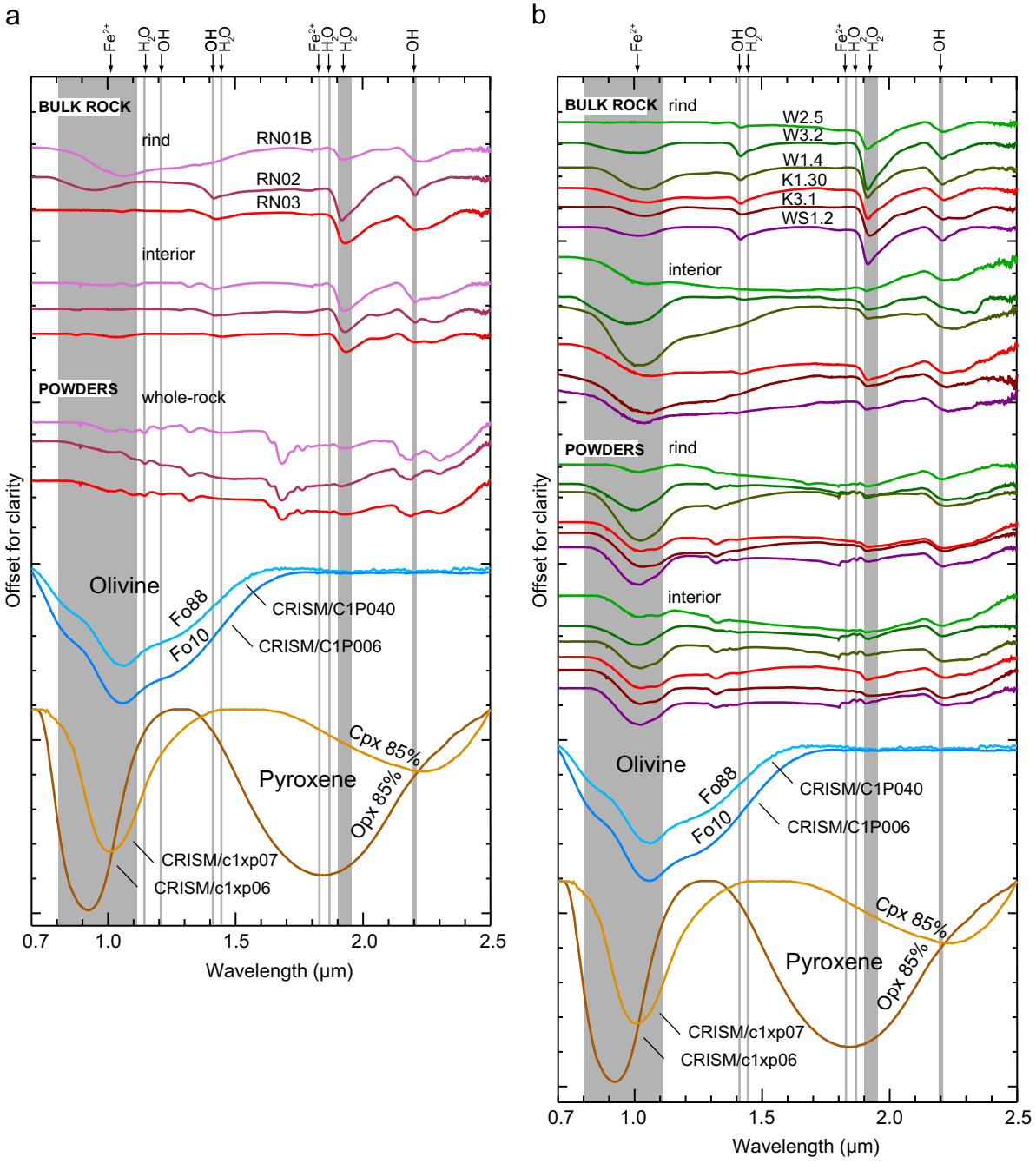

Fig. 5. Representative, continuum removed reflectance spectra of the Ogaden basalts (a), Udokan basalts (b), and library spectra of the iron-rich primary minerals of basalt in the range 0.7–2.5 μm. Spacing of major tick marks on vertical axis is 0.6. The location of the Fe^{2+}, −OH, and H_2O absorption bands discussed in the text is indicated. Continuum (on this figure and the following ones) was removed using the standard ENVI procedure, in which a convex hull is fit over the top of a spectrum using straight-line segments that connect local spectra maxima (Clark and Roush, 1984); "rind" refers to spectra of the surface of the alteration rind, "interior" refers to spectra of the internal, fresher rock, and the sample IDs are according to Table 1.

4. Results

Representative reflectance spectra of the Ogaden and Udokan basalts in the spectral range from 0.7 to 2.5 μm are shown on Fig. 5a, b. Fig. 6 gives a synthesis of the absorption bands observed in the studied basalt spectra. The deepest absorptions are observed in the spectra of the bulk rock rind surface. The spectra of the internal part of the bulk rocks are attenuated, indicating a decreasing influence of alteration minerals on the spectrum, as interpreted by Hunt et al. (1974) on powders and Cloutis (1992) on bulk rock samples. The spectra of the powders show more spectral features than bulk rock spectra. There is no significant difference in the spectra of powders of the rind surface and internal part of the Ogaden samples. This indicates that the level of alteration cannot be inferred from differences in absorption band depth.

4.1. Primary minerals

The primary minerals: olivine, pyroxenes, and plagioclases, were identified using polarized light microscopy (Fig. 3), X-ray diffractometry (Supplementary Fig. 1), and micro-Raman spectroscopy (Fig. 7). Microscopic observations and planimetric analysis (up to 700 counting points in each thin section) revealed that the amount of plagioclase varies between 34% and 44% in the Ogaden

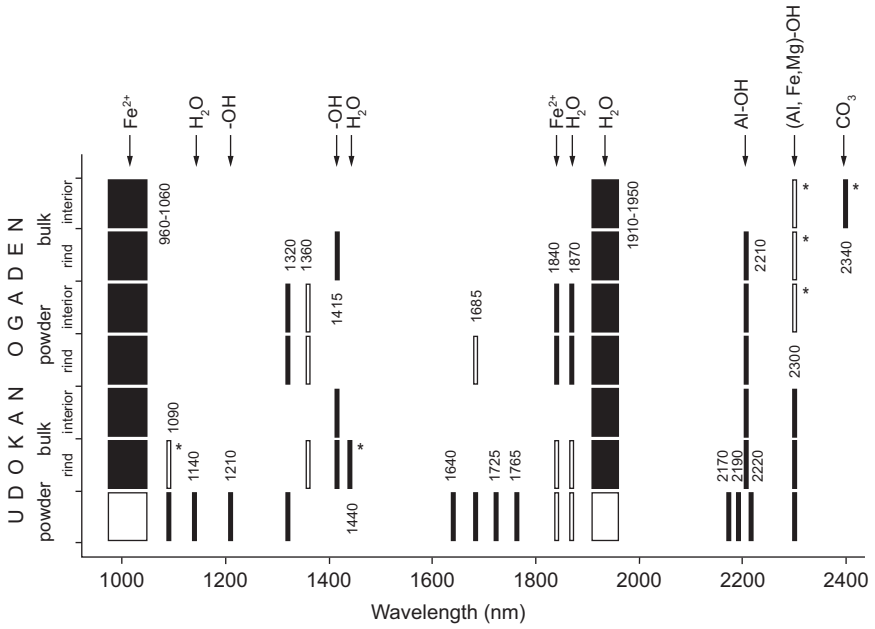

Fig. 6. Synthesis of absorption bands identified in the Udokan and Ogaden basalt spectra. Bar width reflects the range of observed band. Empty bar indicates either very narrow or very shallow band. Star (*) indicates band identification in one spectrum only.

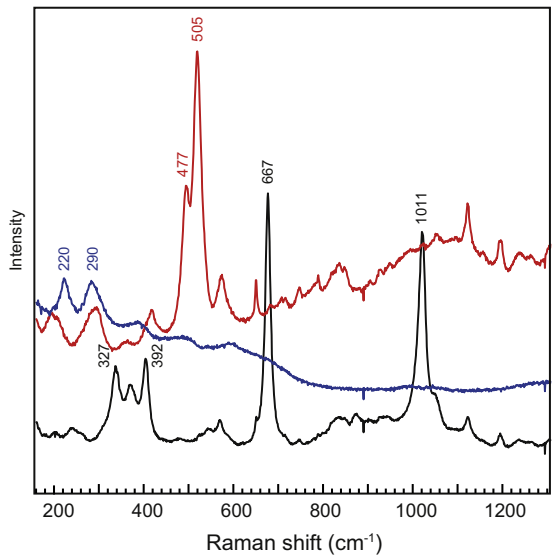

Fig. 7. Representative Raman spectra of the Werder basalt from Ogaden (sample W3.2). In addition to observed fundamental vibrations of plagioclases (477 and 505 cm^{-1}) and clinopyroxenes (327, 392, 667 and 1011 cm^{-1}), there are the bands around 220 and 290 cm^{-1}, which could be the evidence of poorly crystallized hematite, probably mixed with clay minerals.

basalts, while in the Udokan basalts plagioclase participation is more variable, ranging from 24% (sample RN03) to 50% (sample RN01). The most abundant in olivine (17%) is sample W1.4 from Werder (Ogaden). In other basalts, olivine constitutes 2–11% of the sample. The amount of pyroxene is different in each sample, varying from 5% to 29 % in the Ogaden basalts and from 7% to 21% in the Udokan basalts. The iron-bearing primary minerals are also identified using ASD, by the characteristic ferrous iron absorption band around 1.0 μm. This band, usually the only absorption measured on unaltered basalt (Hunt et al., 1974), is observed in both Udokan and Ogaden basalt spectra (Fig. 5). In the Ogaden basalts, iron absorption at ~1 μm is deeper in spectra of the internal part of the bulk rock than in the spectra of the rind surface. This difference disappears in powders (Fig. 5a). In the Udokan basalts, this absorption band is generally absent, apart from bulk rock rind surface spectra, for which two of the three samples display a broad but weak absorption (Fig. 5b).

4.2. Water and hydroxide bands

The absorption band of H_2O at 1.91–1.95 μm is a salient feature of the bulk rock spectra of the Udokan and Ogaden basalts (Figs. 5 and 6). The 1.44 μm H_2O absorption band appears in these spectra occasionally. Basalt powder spectra reveal the 1.91–1.95 μm hydration band only. This band is systematically attenuated compared to the band observed on the corresponding bulk rock spectra.

The three –OH absorption bands centered at 1.41, ~2.2, and ~2.3 μm are diversely observed (Figs. 5 and 6). The 1.41 μm band is usual in the spectra of the bulk rock surface, is attenuated in the spectra of the bulk rock interior, and disappears in the powders. The ~2.2 μm absorption is observed in most spectra. The ~2.3 μm absorption is common in the Udokan basalt spectra, but rare in the Ogaden basalt spectra. Other combinations of fundamental vibration modes (Hunt, 1977) are observed at 1.135 and 1.875 μm. These absorption bands are characteristic of hydrated materials and may be due to a variety of mineral classes, such as clay minerals, hydroxides and zeolites.

4.3. Phyllosilicates

X-ray diffraction demonstrates the presence of clay minerals in the studied samples, indicated by peaks at the low angles 2Θ (Table 3). From the intensity of the clay minerals peaks, the clay content of the Ogaden basalts is higher in the internal part of the samples than at the rind surface. The values of the clay peaks (d values between 13 and 15 Å) indicate smectites. There is no evidence for smectites on X-ray diffractograms for most of the Udokan basalt samples, which might suggest either lack of clay minerals in these samples or (more likely) that the amount of smectites in the samples is too low to be detected using X-ray

Table 3
Mineral phases due to alteration identified in the Udokan and Ogaden basalt samples and methods of identification: M – macroscopically/polarized light microscopy, NIR – near-infrared spectroscopy, R – Raman spectroscopy, XRD – X-ray diffractometry.

Secondary mineral phases	*Udokan*				*Ogaden*					
	RN01A/B	RN02	RN03	RN04	K1.30	K3.1	W1.4	W2.5	W3.2	WS1.2
Phyllosilicates										
Clays (smectites[a])	NIR	NIR	NIR	XRD, NIR	XRD, NIR	XRD, NIR	NIR	NIR	XRD, NIR	XRD, NIR
Iddingsite	M, NIR	M, NIR	M, NIR	M, NIR	M, NIR	M, NIR	M, NIR	M, NIR	M, NIR	M, NIR
Iron oxides and hydroxides										
Ferrihydrite		XRD, NIR	XRD, NIR							
Hematite									R	
Zeolites[b]	M, NIR	M, NIR	M, XRD, NIR	M, NIR						
Carbonates										
Calcite	M, NIR	M, NIR	M, NIR	M, NIR			M, NIR	M, NIR	M, NIR	

[a] Smectites: montmorillonite, nontronite, beidellite, saponite, hectorite.
[b] Zeolites: analcime, natrolite, clinoptilolite, chabazite.

diffractometry, as the detection limit of this technique is around 5% (Moore and Reynolds, 1997).

Near-infrared spectra of the Ogaden and Udokan basalts systematically display absorption bands of two smectites, montmorillonite and nontronite (Fig. 8, Table 4). Montmorillonite has a deep 2.20 μm absorption band due to Al–OH bend plus –OH stretch; this band almost disappears in nontronite spectrum, in which –OH stretch plus an Fe–OH bend result in a deep absorption band at 2.28–2.32 μm (Clark et al., 1990). Most spectra of the Udokan basalt bulk samples and powders display absorption bands at 2.21 and 2.30–2.31 μm, consistent with the presence of both minerals. In all the spectra of the rind surfaces of the Ogaden samples, only montmorillonite is observed, and corresponds to the clay that accumulates in pans (Fig. 2g). Udokan basalt powder spectra show an absorption band at 2.19 μm instead of 2.21 μm (Fig. 8), which may denote a higher Al content than pure montmorillonite, and crystallization of beidellite instead of montmorillonite (Bishop et al., 2010). The 1.14 μm absorption band, a water combination tone (Hunt, 1977), observed in all the Udokan basalt powder spectra may also be related to the presence of montmorillonite or nontronite (Fig. 8, Table 4). Alternatively, the 1.14 μm band could be due to the presence of other smectites such as saponite, which often settles in basalt vesicles under hydrothermal processes (April and Keller, 1992; Anthony et al., 2003), or hectorite, which forms by alteration of volcanic rocks containing clinoptilolite (Anthony et al., 2003), a zeolite that is suspected to be present in the Udokan basalt vesicles (see Section 4.5). However, those smectites also absorb at 2.39 μm, a band which is not observed in any of the studied spectra.

In all the studied basalt samples, olivine is partly replaced by iddingsite (Fig. 4, Table 3). This process is the most prominent in samples from Udokan, especially RN02 and RN03, where the amount of iddingsite reaches 34% and 50%, respectively. Iddingsite is almost featureless in the NIR range investigated in this study, apart from the hydration band around 1.90 μm, as previously noted by Cloutis (2004). However, in addition to the absorption at 1.90 μm, weak absorptions and slope variations in the continuum removed spectrum of iddingsite CRISM/IDD001 (PDS Geosciences Spectral Library Service) are systematically observed in the continuum removed spectra of the Ogaden, and, to a lesser extent, the Udokan basalt powders.

4.4. Iron oxides and hydroxides

X-ray diffractometry suggests the presence of ferrihydrite in the Udokan basalts. This result is consistent with the absorption bands at 1.41–1.44, 1.76, and 1.91–1.95 μm observed in the NIR spectra (Fig. 9, Tables 3 and 4). However, ferrihydrite, as well as iron hydroxides, cannot be identified in the studied NIR spectra unequivocally, because their absorption bands, due to Fe^{2+}, –OH, and H_2O, are not diagnostic when they are associated with other water- and iron-bearing minerals. Ferrihydrite might be an interlayer component of Fe^{3+}-enriched smectites (Bishop et al., 1993), but it is also a possible constituent of iddingsite (in SNC meteorites; Treiman et al., 1993; Treiman and Lindstrom, 1997), increasing the likelihood that the observed X-ray peaks correspond to ferrihydrite, given that iddingsite has been identified in large quantities in thin sections (Figs. 3 and 4).

Bands around 220 and 290 cm^{-1} in the Raman spectrum of the Werder basalt from Ogaden (Fig. 7) might be attributed to poorly crystallized hematite, probably mixed with clay minerals. They may also correspond to iddingsite (Kuebler, 2013).

4.5. Zeolites

Minerals from the zeolite group were identified in Udokan basalt vacuoles, both macroscopically and using a polarizing microscope (Table 3). However, absorption bands of pure zeolites do not match the absorptions observed in the Udokan basalt spectra, nor the spectrum of a zeolite mixture in Oregon basalt (Fig. 10). Pure natrolite from the Deccan traps (USGS/HS169.3B, Fig. 10) has absorption at 1.19 μm instead of 1.14 μm. Analcime, which has been independently identified in Udokan basalt using XRD, is not satisfactory either if considered alone. In particular, the 2.2 μm absorption band, characteristic of both the Udokan basalt spectra and the spectra of other zeolites, is absent in the analcime spectrum, which displays an absorption band at 2.13 μm instead (Fig. 10).

The near-infrared spectrum of a zeolite mixture that crystallized in vesicles of a basalt from Springfield, Oregon (Clark et al., 1990, 2007), displays five absorption bands that match absorption bands of the Udokan basalt powder spectra: 1.14–1.15, 1.76, 1.91–1.94, and 2.19 μm (USGS/168.3B, Fig. 10), all resulting from absorption by H_2O molecules within the zeolite cavities (Clark et al., 1990). Thin section analysis has revealed that this mixture includes 40% natrolite, 30% analcime, and 20% of clinoptilolite, and is associated with 10% calcite (Clark et al., 2007). Note that the

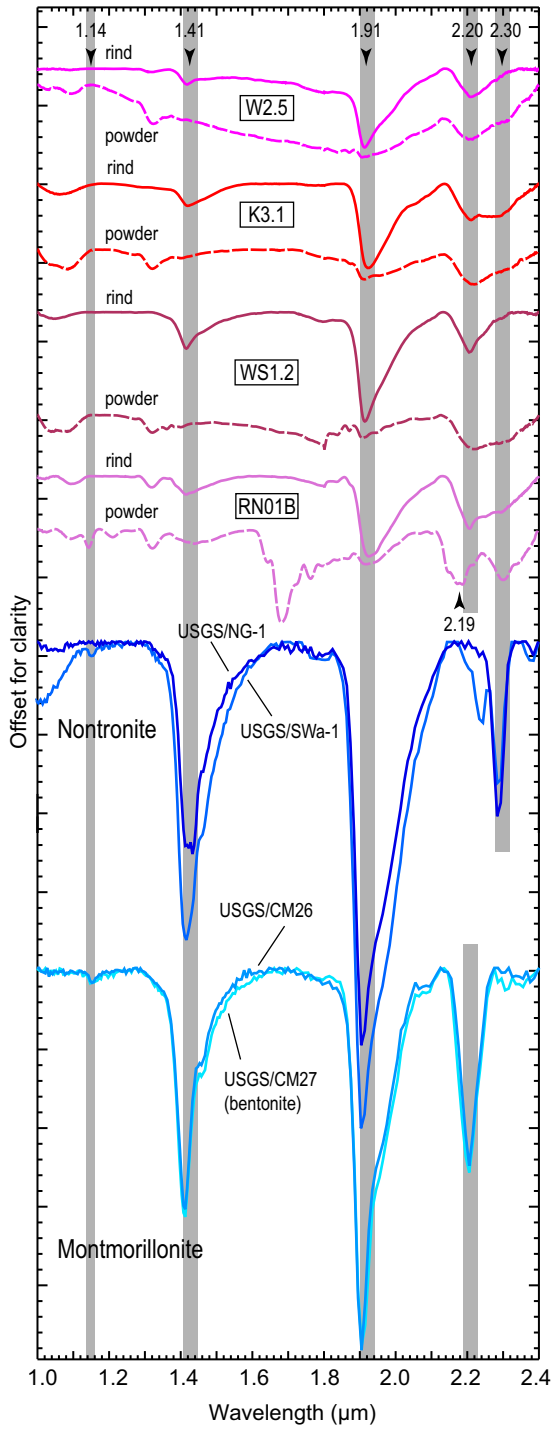

Fig. 8. Continuum removed reflectance spectra of the Ogaden and Udokan basalt rind surfaces and powders, and library spectra of montmorillonite and nontronite in the range 1.0–2.4 μm. Spacing of major tick marks on vertical axis is 0.11. The gray lines indicate absorption bands common to the basalt spectra and the library spectra.

1.14 μm absorption band may deepen smectite absorption at the same wavelength (Fig. 8).

Another zeolite mixture that matches absorption bands observed in the Udokan basalt powder spectra is a sub-equal proportion of chabazite, thomsonite, and wairakite (wairakite forms a solid solution with analcime). A hydrothermal alkaline suite, in which these three minerals are zoned with depth in various volcanic rocks (Cole and Ravinsky, 1984), has several absorption bands in common with the Udokan basalt powder spectra: 1.15, 1.73, 1.76, and 1.91 (Fig. 11).

The zeolites observed in the Udokan basalts are therefore best interpreted to be a mixture, which is common in volcanic rocks (e.g., Chipera and Apps, 2001). The candidates to the mixture in the Udokan basalts are analcime, natrolite, clinoptilolite, and chabazite.

4.6. Carbonates

Carbonates of fumarolic origin, either filling vesicles or veins, are systematically observed in the thin sections of the Werder basalt samples (Table 3). Nevertheless, only limited evidence of carbonates is found in the spectra. The complexity of the mineralogical assemblage may mask or strongly attenuate the most prominent carbonate absorption band at 2.33–2.34 μm (Gaffey, 1986) (Fig. 12). The library spectrum of sample USGS/HS168.3B in Fig. 10 is an example where this absorption is missing despite the 10% calcite identified by XRD. The other carbonate absorption bands in the studied NIR range are located at 1.75–1.76, 1.87–1.88, 1.97–2.00, and 2.17–2.18 μm (Gaffey, 1986). In the Werder basalt powder spectra, the only indication of carbonates is a systematic absorption band at 1.87 μm (Fig. 12, Table 4).

The carbonates observed in the Udokan basalt samples (Table 3) do not show any prominent spectral signature at 2.33–2.34 μm either; nevertheless, the absorption band systematically observed at 1.76 μm on the spectra of the Udokan basalt powders may be due to calcite (Fig. 12, Table 4), in addition to H_2O absorption by zeolites (Fig. 10). Very shallow bands observed at 1.87 and 2.17 μm might also indicate carbonates. The absence of a definitive spectral signature of carbonates is interpreted to result from the nonlinear spectral response of intimately mixed minerals found in basaltic rocks (Hapke, 1993). Mineral optical properties, as well as relative grain size and mineral abundance, especially in the complex weathering context, can mask some mineral components and overrepresent others (Chevrier et al., 2006; Cloutis et al., 2010), and carbonates are likely underrepresented in the Udokan basalt spectra.

4.7. Contaminating materials

Some absorption bands in the Udokan basalt powder spectra cannot be reconciled with any mineral that may form by alteration of basalt. Natural as well as anthropic processes may influence the spectral signature. The rock samples were indeed not cleaned prior to analysis in order not to remove or damage alteration products, leaving the possibility of spectral contamination.

The rock samples may be contaminated from the lichen *Cladonia rangiferina* (Afonin et al., 2008), which develops on the Udokan basalts (Fig. 2b), or from Dahurian larch *Larix dahurica* (*L. gmelinii*) (Tchebakova et al., 2005; Malyshev et al., 2008; SRK Consulting, 2010), which is the main local tree species in the forest where the Udokan volcanics are located (Fig. 2a). As shown on Fig. 13, the absorption bands of sap coincide with the 1.64, 1.68, 1.73, and 1.76 μm absorptions in the Udokan basalt powder spectra. The 1.73 μm absorption is attributed to terpenes (Elvidge, 1990), and the 1.68, 1.73 and 1.76 μm absorptions correspond to the first overtone of C–H stretch (Miller, 2001). Absorptions at 1.13 and 1.19 μm in sap, due to the combination tone of water (Hunt, 1977) and an O–H bending overtone (e.g., Curran, 1989; Elvidge, 1990), respectively, may be analogous to the 1.14 μm and 1.21 μm absorptions in the Udokan basalt powder spectra. Comparison between the NIR spectra of Udokan basalts and *Cladonia rangiferina* also reveals common water and OH absorptions; however the overall spectrum does not match the basalt spectra. A more detailed comparison between the Udokan basalt powder spectra and the spectra of debris expected in the Udokan sampling sites

Table 4
Absorption bands and corresponding mineral phases due to alteration identified in the Udokan and Ogaden basalt spectra

Absorption band (μm)	*Secondary mineral phases*	*Udokan*				*Ogaden*					
		RN01A/B	RN02	RN03	RN04	K1.30	K3.1	W1.4	W2.5	W3.2	WS1.2
1.14	Smectites, zeolites	•	•	•	•						
1.41–1.44	Smectites, ferrihydrite, zeolites	•	•	•	•	•	•	•	•	•	•
1.73	Zeolites	•	•	•	•						
1.76	Ferrihydrite, zeolites, calcite	•	•	•	•						
1.87	Smectites, zeolites, calcite	•	•	•	•	•	•	•	•	•	•
1.91–1.95	Smectites, iddingsite, ferrihydrite, zeolites	•	•	•	•	•	•	•	•	•	•
2.17	Calcite	•	•	•	•						
2.19	Beidellite, zeolites	•	•	•	•						
2.21–2.22	Montmorillonite, zeolites	•	•	•	•	•	•	•	•	•	•
2.30	Nontronite, zeolites	•	•	•	•	•	•	•	•	•	•
2.34	Calcite	•								•	

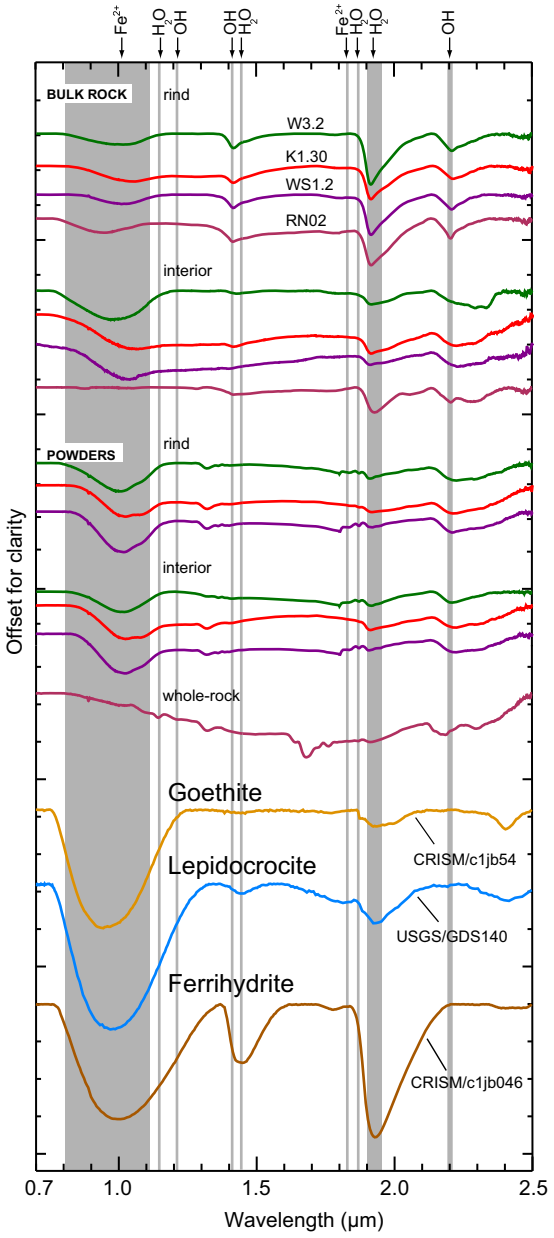

Fig. 9. Selected, continuum removed reflectance spectra of the Ogaden and Udokan basalts, and library spectra of ferrihydrite and hydroxides in the range 0.7–2.5 μm. Spacing of major tick marks on vertical axis is 0.6. The location of the Fe^{2+}, –OH, and H_2O absorption bands discussed in the text is indicated.

(cones, needles, bark, cellulose, lignin, and arabinogalactan, an abundant larch wood polysaccharide) is given in Supplementary Fig. 2.

Another possible source for the 1.68, 1.73 and 1.76 μm C–H stretch overtone observed in the Udokan basalt powder spectra may be polycyclic aromatic hydrocarbons (PAHs) (Izawa et al., 2014). Forest fires, frequent in Siberia during summer, are a known source of PAHs emission. Another source of this emission can be industrial activities. The Udokan sampling site is located near the copper mine, which releases a variety of PAHs, especially at the KM28 site (SRK Consulting, 2014), located 25 km away from Udokan basalt sampling sites. The Udokan basalt powder absorptions at 1.14, 1.64, 1.68, 1.73, and 1.76 μm may include a contribution from various types of PAHs (Izawa et al., 2014) (Supplementary Fig. 3).

5. Discussion

5.1. Comparison between bulk rock spectra

Most spectra of the internal part of the bulk rocks are broadly similar, with the usual broad Fe^{2+} absorption band at ~1 μm (Fig. 14). Two Udokan basalt spectra do not show this absorption band (thick black lines on Fig. 14), as was also noted on some basalts investigated by Hunt (1977); this is consistent with thin section observations indicating that the samples are not ideally fresh.

The basalt rind surfaces display deeper absorption bands than the internal parts of the samples (Figs. 14 and 15). The differences between the Udokan and Ogaden basalt spectra are usually minor. For instance, the spectra from Kebri Dehar sample K3.1 from Ogaden and RN01B from Udokan are almost duplicates in the range 1.7–2.4 μm, and K1.30 is almost parallel to RN02 (Fig. 15). It appears, therefore, that different weathering conditions studied here do not produce different bulk rock spectra. This is true for the hot (Ogaden) versus cold (Udokan) climates, but is also true in the hot environment for samples with different weathering histories, including polyphase (Kebri Dehar and Werder samples). The polyphase case, illustrated in Fig. 16a shows that in the absence of pedogenesis, a drying environment 'fossilizes' the alteration features of the earlier environment because the weathering rind that develops is thinner than the earlier-formed rind. In such a case, if the NIR spectra of the basalt rind surface and the internal part of the sample are similar, then it must be concluded that different environment conditions cannot be predicted from NIR spectra. In the case of a more complex weathering history, in which dry and wet climate alternate several times (successions of the scenarios

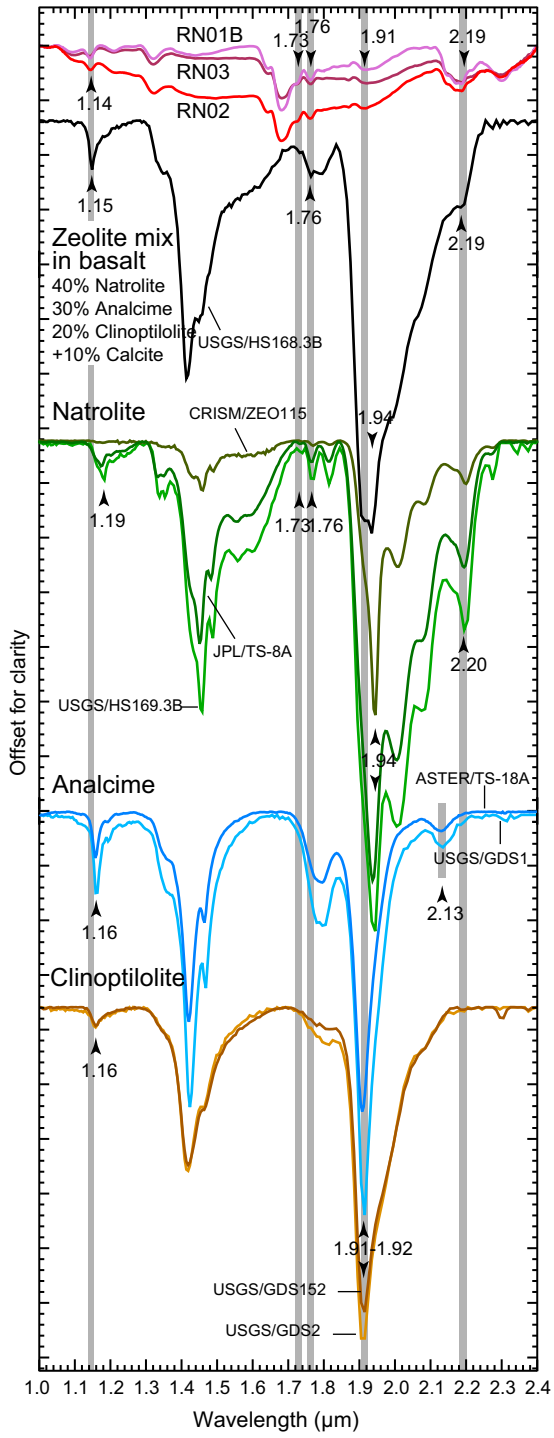

Fig. 10. Continuum removed reflectance spectra of the Udokan basalt powders, spectrum of the zeolite mixture in Oregon basalt (Treiman and Lindstrom, 1997), and library spectra of zeolites in the range 1.0–2.4 μm. Spacing of major tick marks on vertical axis is 0.105. Both the Udokan and Oregon basalt spectra display absorption bands at 1.14–1.15, 1.76, 1.91–1.94, and 2.19 μm. The match between the spectra of pure minerals of this zeolite mixture and the Udokan basalt spectra is poorer.

depicted in Fig. 16a and b), the weathering rind produced in a wet environment is expected to systematically overprint evidence of any earlier drier environments, the weathering rind of which is systematically destroyed or deeply modified by the next rind. It is unlikely that a complex weathering history leads to a complex weathering record in the samples, because the older weathering record is gradually removed from the samples surface as soon as

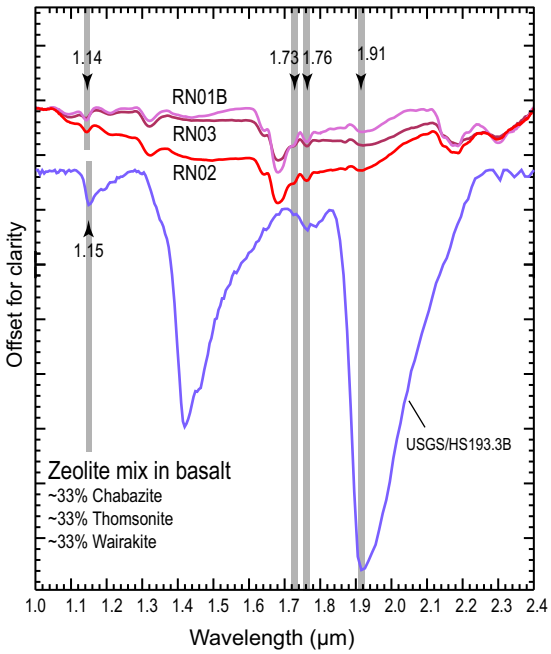

Fig. 11. Continuum removed reflectance spectra of the Udokan basalt powders and library spectra of a mixture of chabazite, thomsonite, and wairakite, in sub-equal proportions (Treiman and Lindstrom, 1997) in the range 1.0–2.4 μm. Spacing of major tick marks on vertical axis is 0.105. The absorptions observed at 1.15, 1.73, 1.76, and 1.91 are also observed in the Udokan basalt spectra.

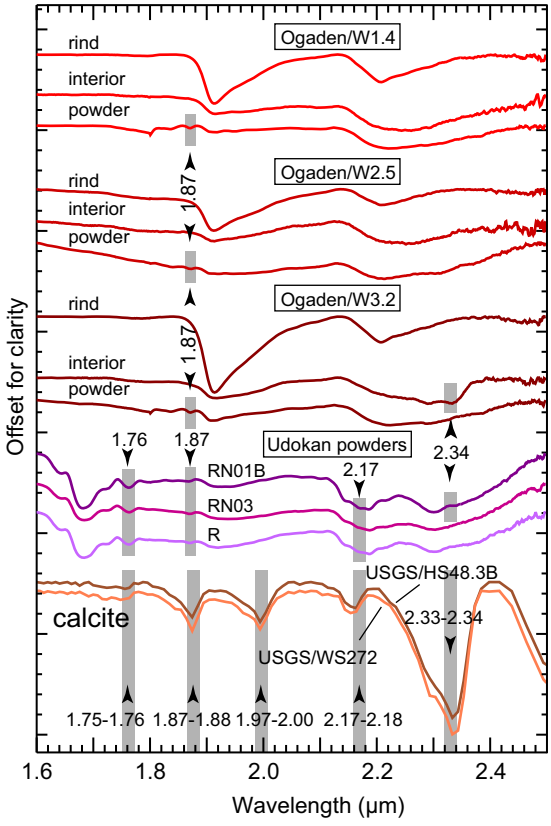

Fig. 12. Continuum removed reflectance spectra of the Werder basalts from Ogaden, the Udokan basalts, and library spectra of pure calcite in the NIR range of the diagnostic absorption features of carbonates. Spacing of major tick marks on vertical axis is 0.225. The band centers of calcite are given after Gaffey (1986). Although there is an evidence of calcite in the Werder basalt samples from thin sections, it is usually not identifiable in the spectra; other minerals mask most or all of the diagnostic absorptions of calcite. The zeolites identified in the powder of the Udokan basalt samples may be associated with a small amount of carbonate.

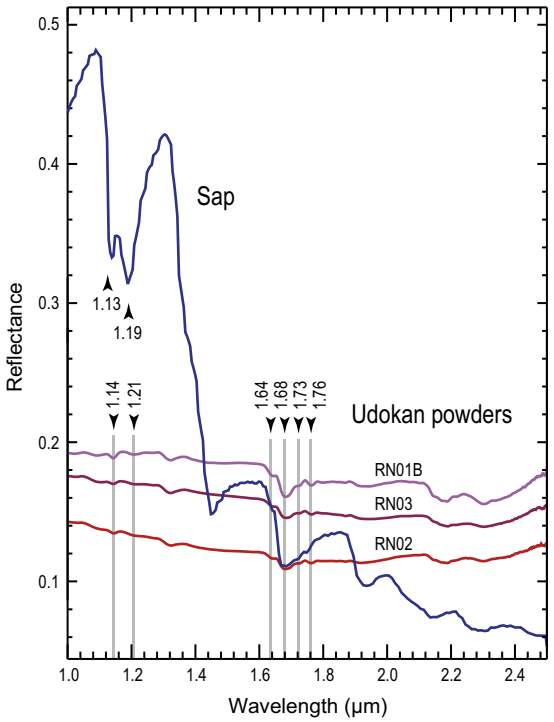

Fig. 13. Reflectance spectra of the Udokan basalt powders and library spectrum of sap (Elvidge, 1990) in the range 1.0–2.5 μm. The gray lines indicate absorption bands common to the basalt and sap spectra.

the surface looses cohesion and the alteration products are transported downstream.

The H_2O absorption band observed at 1.9 μm in the spectra of the weathering rinds is usually deeper for the Ogaden basalt (Fig. 15). The Ogaden basalt spectra reflect the present dry environment, which is drier than the Udokan environment, where freeze/thaw cycles seasonally occur. Thus, an inverse correlation exists in this dataset between hydration band depth and humidity of the sample environment.

5.2. Comparison between basalt powder spectra

Analysis of basalt powder spectra allowed identification of significantly more secondary minerals than analysis of the bulk rock spectra, and more accurately. Many small absorption bands and the spectral slopes that appear in the powder spectra in the NIR range were not observed in the bulk rock spectra (Fig. 17).

Similarities between the Ogaden and Udokan basalt powder spectra (Table 5) are: (1) the ~1.4 μm –OH band observed on the bulk rock spectra becomes significantly weaker (Udokan) or even disappears (Ogaden) in the powders, probably due to dehydration; (2) the broad ~1.9 μm H_2O band that dominates the bulk rock spectra becomes narrower and much shallower, revealing the 1.87 μm H_2O absorption and the positive spectral slope between ~1.8 and ~1.9 μm; (3) the presence of montmorillonite and nontronite, with clearer evidence of nontronite in the Udokan basalt spectra, (4) the presence of iddingsite.

In contrast to the bulk rock spectra of the Ogaden and Udokan basalts, the powder spectra show the following differences (Table 5): (1) in the Udokan basalt powder spectra, the broad Fe^{2+} 1 μm absorption band almost disappears, whereas in the Ogaden basalt powder spectra it remains essentially unaffected by alteration; (2) zeolites are observed in the Udokan samples only; (3) the spectral slope of the Udokan basalt powder spectra from 0.9 μm toward the longer wavelengths is negative at first-order, whereas it is positive in the Ogaden basalts powder spectra (Fig. 17).

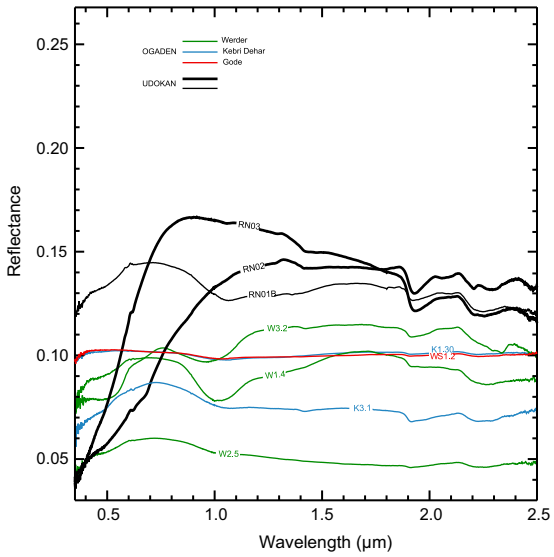

Fig. 14. Comparison between reflectance spectra of the Ogaden and Udokan fresh or nearly fresh rock surfaces. The spectra are nearly similar, apart from the missing ~1 μm absorption in two of the Udokan basalt spectra (thick black lines).

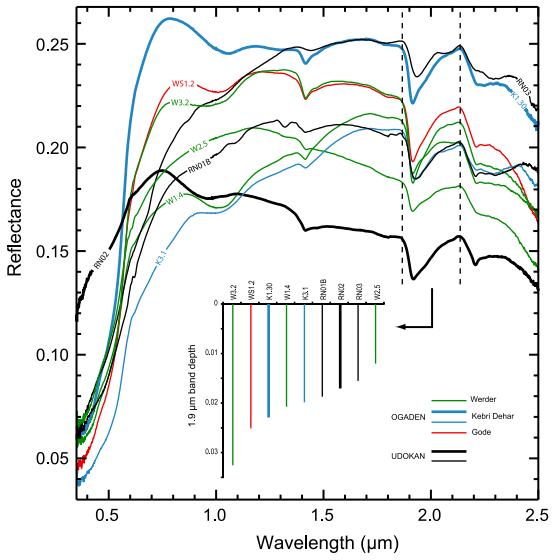

Fig. 15. Comparison between reflectance spectra of the Ogaden and Udokan basalt rind surfaces. Note the parallel spectra of the Udokan sample RN02 and Ogaden sample K1.30 in the range 0.7–2.5 μm (thick lines), and the nearly identical spectra of the Udokan sample RN01B and Ogaden sample K3.1 in the range 1.9–2.4 μm. Water absorption band at 1.9 μm is almost always deeper in the Ogaden than in the Udokan basalt spectra, as detailed in the inset, where the band depth is calculated by subtracting from each spectrum a convex continuum hull between 1.88 and 2.13 μm, following the method presented by Morris et al. (1982).

Spectral slope depends on both the grain size and optical properties of the minerals, both of which influence scattering (Hapke, 1993; Hiroi and Pieters, 1994; Harloff and Arnold, 2001). However, all the powders were ground to the same particle size, indicating that this difference in spectral slope more likely reflects differences in alteration conditions rather than physical differences in sample preparation; (4) existence of vegetal material in the Udokan basalt samples.

Zeolites are, therefore, the only secondary minerals that might explain the differences due to alteration between the Ogaden and Udokan basalt powder spectra. Their identification is a major indicator of ancient presence of water, whether of groundwater or hydrothermal activity origin. The restrictive pressure and

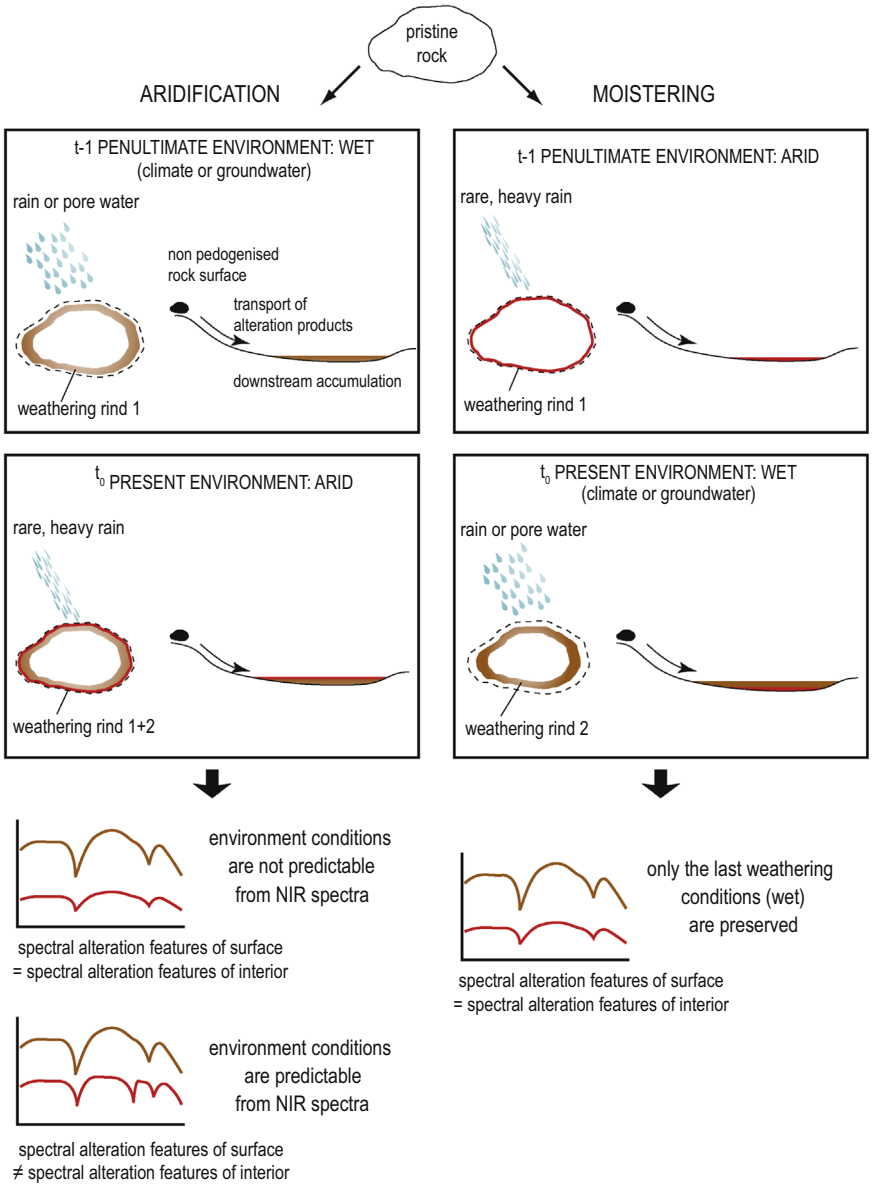

Fig. 16. Interpretation of NIR spectra of bulk rock in case of successions of contrasting weathering conditions: from wet to dry (a) and from dry to wet (b). For all studied samples, the present situation is (a), and the similar spectra of the alteration rind and interior of the sample indicate that environment conditions cannot be retrieved from analysis of the NIR spectra.

temperature range of formation of some zeolites potentially helps in retrieving information on paleoclimate.

5.3. *Smectites versus zeolites*

Most spectra, whether of bulk rock or powder, display absorption bands around ~2.2 and 2.3 μm. These absorptions are usually assigned to combinations of –OH stretch and Al–OH or Fe, Mg–OH bend, respectively. In altered basalt, they are usually interpreted as due to montmorillonite and nontronite. However, in the Udokan basalt powder spectra, the single 2.20–2.21 μm absorption band observed in bulk rock spectra is replaced by a band centered at 2.19 μm, associated with two smaller bands or shoulders located at 2.17 and 2.22 μm (Fig. 8). The 2.17 and 2.19 μm absorptions could be related to the presence of zeolites (Fig. 10) and calcite (Fig. 12), respectively. Some zeolites also absorb the 2.3 μm wavelength (Fig. 10). In the Ogaden basalt spectra, the absence of 1.14 μm band, which is a combination of fundamental modes of H_2O vibrations (Hunt, 1977), could be due to a slightly different smectite hydration state or to the absence of zeolites. The signature of many zeolite mixtures may, therefore, be confused with the signature of montmorillonite and nontronite. This can happen especially if the spectral noise is high, which is often the case with Martian surface spectra.

On the Werder basalt spectra of Ogaden, the absorption band around 2.2 μm (Fig. 8) might also not be fully due to montmorillonite. The difference between the intensity of the plagioclase peaks on the diffractograms of the alteration rind and internal part of the sample is indeed not correlated with the intensity of the clay peaks, confirming that basalt alteration does not occur significantly through clay formation in these samples.

5.4. *Implications for Mars*

The studied spectra are not directly compared to the particular spectra of Martian surface obtained by OMEGA and CRISM spectrometers. Comparing against OMEGA spectra would be of limited interest due to their low resolution (100 m/pixel). The CRISM

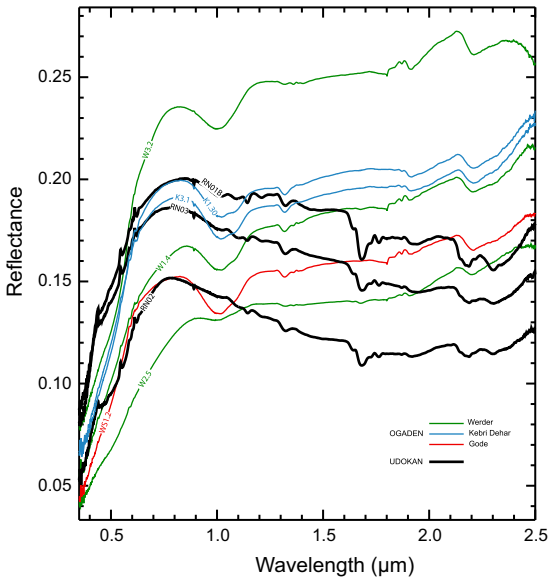

Fig. 17. Comparison between reflectance spectra of the Ogaden and Udokan basalt powders. Several spectral features, that are not apparent in bulk rock spectra, appear. The powder spectra of basalts altered in arid hot environment (Ogaden) show a first-order positive spectral slope in the range 0.9–2.0 μm, whereas spectra of basalts altered in arid cold environment (Udokan) have a first-order negative spectral slope.

Table 5
Similarities and differences between the Udokan (arid cold environment) and Ogaden (arid hot environment) basalt powder spectra.

Feature	*Udokan*	*Ogaden*
Broad Fe^{2+} 1 μm absorption band	Almost full disappearance	Essentially unaffected by alteration
~1.4 μm –OH band observed on the bulk rock spectra	Weakening	Disappearance
~1.9 μm H_2O band observed on the bulk rock spectra	Band narrowing and shallowing	
Montmorillonite/nontronite	Yes	Yes
Iddingsite	Yes	Yes
Zeolites	Yes	No
Spectral slope 0.9–2.0 μm	Negative	Positive

spectra of Martian rocks interpreted to be basalts (Salvatore et al., 2010) do not show any alteration bands, therefore they cannot be compared to the altered basalt spectra presented here (Figs. 15 and 17). The CRISM spectra that display absorption bands of alteration minerals are attributed to mafic rocks in general, not basalts specifically (e.g., Mustard et al., 2008).

5.4.1. *In situ altered basalt or clay deposits?*

All the studied samples are from basaltic solid rock. The products of *in situ* rock alteration are redeposited at a lower topographic level; for example, in the Ogaden, typically in pans after heavy rains, such as on Fig. 2g. Nevertheless, the spectral signature of smectites, especially montmorillonite, is prominent in all the samples, including the alteration rind surfaces (Figs. 5 and 8). The internal, fresher part of samples also display signatures of alteration to smectites, though attenuated compared to the spectra of the rind surface (Fig. 5). As a consequence, identification of smectites on spectral datasets of Mars obtained in orbit is not an evidence of sedimentary accumulation of clay minerals or *in situ* pedogenesis; even only slightly altered basalts have spectra displaying clear absorption bands of smectites.

5.4.2. *Use of clay-sized fraction to retrieve alteration conditions*

From the interpretation of the studied samples, it must be inferred that analysis of the NIR spectra of Martian bulk rocks is unlikely to help distinguish between basaltic rocks that were altered in hot or cold arid environment. This study suggests, however, that analysis of rock powders can help in identifying alteration due to weathering, groundwater, or hydrothermal activity because of the presence of zeolite signature. In addition, the opposite slope of the NIR spectra between 0.9 and 2.0 μm for these contrasted alteration conditions (Fig. 17, Table 5) could not be explained. Although grain size affects spectral slope, this is unlikely to be the cause of these opposite slopes since all the samples were ground to the same grain size. This leaves open the possibility that their origin is related to the environmental conditions of alteration.

5.4.3. *Depth of hydration band and climate aridity*

The Ogaden basalts are located in a much more arid setting than the Udokan basalts but hydration bands are deeper in the Ogaden basalt spectra than in the Udokan basalt spectra (Fig. 15). This inverse correlation observed between the depth of the hydration bands and climate aridity may be related to the weathering effect of groundwater, or to the hydration state of the secondary minerals. Therefore, the deep hydration bands observed on many Martian spectra of mafic mineral-rich areas (Mustard et al., 2005), and maybe also those observed in other geological contexts (e.g., Bishop et al., 2008; Mustard et al., 2008), are not necessarily the evidence of a past wet climate characterized by persistent water runoff during long-lasting wet seasons. They are also consistent with dry conditions, cold or hot, with only very limited or no precipitation.

Similarly, nontronite is frequently indicative of alteration of mafic or ultramafic rocks in water-saturated or marine conditions (Anthony et al., 2003), or in association with biogenic activity at hydrothermal sources (Köhler et al., 1994), leading to the interpretation that its existence on the Martian surface proves the existence of liquid H_2O (McKeown et al., 2009). However, nontronite has also been observed to form within cracks in a basaltic cobble in a dry and cold environment in Greenland (Bender Koch et al., 1995).

5.4.4. *Evidence for carbonates and iddingsite on Mars*

Although carbonates are rarely detected in the orbital NIR spectra of the Martian surface (Ehlmann et al., 2008), their presence at the surface is suggested from Mars Exploration Rover Mössbauer spectrometer and mini-TES data (Morris et al., 2010), and carbonate decomposition products have been possibly identified using Mars Global Surveyor TES data (Glotch and Rogers, 2013). Carbonates could not be reliably identified also in the NIR spectra studied here (Fig. 12), which is interpreted to result from the nonlinear spectral response of intimately mixed minerals found in basaltic rocks.

The presence of iddingsite on Mars has been advocated based on the analysis of the Lafayette nakhlite (e.g., Treiman and Lindstrom, 1997), and taken as an evidence of liquid H_2O in the past (Swindle et al., 2000), either at surface or, more likely, circulating at shallow depth (Treiman et al., 1993). Iddingsite is abundant in both the Udokan and Ogaden basalts, but its featureless signature in the NIR range makes it hardly identifiable in spectra.

5.4.5. *Mineralogy and temperature*

Montmorillonite, which has been identified in many spectra of old terrains of Mars (Poulet et al., 2005; Mustard et al., 2008; Ehlmann et al., 2009; Roach et al., 2010), is frequently considered to form in hot or temperate environments. However, its identification in both the hot Ogaden and cold Udokan environments

(Fig. 8) shows that this mineral is not diagnostic of temperature, as has been discussed by Vogt et al. (2010) in another study of the Lake Baikal area. Montmorillonite, like other expandable clay minerals, is now suspected to form more commonly under cold conditions (Grygar et al., 2005) to such an extent that Vogt et al. (2010) have questioned whether a number of smectite soils in temperate regions on Earth are inherited from colder times.

Poorly crystallized red hematite is widespread and has been advocated as the origin of the red color of the Martian surface (Morris et al., 1997). Red hematite, which has been found as an alteration product of some of the Ogaden basalt samples (Fig. 7), is a widespread alteration product of basalts in tropical regions, but also constitutes a varnish on basaltic cobbles at the summit of Greenland nunataks (Bender Koch et al., 1995). It is, therefore, not diagnostic of temperature of alteration.

At Gusev Crater, the Pancam multispectral camera of the Spirit rover of the MER mission has identified a mineral that could be ferrihydrite, goethite, maghemite, or schwertmannite (Bell et al., 2004). Ferrihydrite is a precursor of poorly crystallized hematite in cold and arid environment, where it is found in association with goethite, maghemite, and magnetite (Bender Koch et al., 1995). It has been found in a similar environment in the Udokan basalt samples (Supplementary Fig. 1), which may have implications for understanding the alteration environment of Gusev Crater as identified by Bell et al. (2004).

5.4.6. *Extrapolation of results from terrestrial samples*

The spectral signature of the Udokan basalt powder sheds lights on unexpected issues for comparative planetary geology. In order to characterize rock alteration it is necessary not to clean the samples chemically prior to analysis, leaving open the possibility of sample contamination by products of natural or anthropic origin. Wood products, PAH emissions from forest fires as well as industrial activities may contaminate samples that could be identified in the 1.6–1.8 μm spectral range, where few minerals absorb. However, absorptions in ranges where both contaminating products and minerals absorb light might lead to erroneous interpretations if enough care is not taken.

6. Conclusions and perspectives

1. Inferring information on paleoenvironment conditions has not been possible from analyses of the NIR spectra of bulk rocks only; it requires analyses of rock powder spectra. The NIR spectra of the Martian bulk rocks obtained *in situ* are, therefore, unlikely to record the differences in environment conditions. Spectral data obtained from orbit usually mix the signal of hard and loose rocks. Interpretation of powder spectra is however made complicated because not only additional minerals may be identified, but also small particles of organic origin may influence the spectral signal.
2. An inverse correlation is observed between the depth of the hydration bands and climate aridity, possibly due to the weathering effect of groundwater, or to the hydration state of the secondary minerals. Therefore, the deep hydration bands, observed on many Martian spectra of mafic mineral-rich areas or in other geological contexts, are not necessarily evidence of a past wet climate characterized by persistent water runoff during long-lasting wet seasons. They are also consistent with dry conditions, cold or hot, with only very limited or no precipitation.
3. Spectra of the bulk rocks that are only slightly altered display clear absorption bands of smectites, especially montmorillonite. Thus, clay minerals detected in NIR spectra of Mars may indicate the presence of a solid basaltic surface with only very minor alteration and it does not unequivocally point to the sedimentary accumulation of basalt weathering products or pedogenesis. Any interpretation of accumulation of clay minerals by sedimentary or pedogenic processes must be supported by other evidence, such as high-resolution imagery or field observations by landers or rovers.
4. Interpretation of zeolites from their NIR spectral signature is not straightforward. One of the diagnostic absorption bands of natrolite, at 2.2 μm, produced by molecular water, can be confused with the 2.2 μm band of the –OH stretch plus Al–OH bend combination in montmorillonite. Similarly, the 2.3 μm absorption of nontronite may be confused with clinoptilolite. Both smectites and zeolites may display absorption at 1.14 μm. Because zeolites commonly occur in basalts, whether of hydrothermal origin or precipitated from groundwater, confusion between zeolites and smectites may appear.
5. Carbonates could not be reliably identified in the NIR spectra studied here, even though they are present in the samples. Carbonate spectral features can be masked by the signature of other minerals if the signal-to-noise ratio is not high enough, and their prominent 2.33–2.34 μm absorption band, commonly used as a clue to their identification, may be lacking. Similarly, analcime, which has been identified in the studied basalts by XRD, has a characteristic absorption at 2.13 μm, which is not observed in any spectra. These observations illustrate that considerable care should be taken in interpreting mineral spectra on Mars from the most prominent absorption bands, whether or not due to H_2O, because rocks are intimate mixtures of minerals, especially when weathered.
6. More generally, interpretation of NIR spectra with extensive control from solid samples of known geologic and climatic context, polarized light microscopy, and XRD, does not remove the ambiguity of a number of absorption features in altered basalt. Most bands can be attributed to secondary minerals of two or more groups.
7. Zeolites, which were found only in basalt samples from the cold environment, have a strong signature in NIR spectra of altered basalt if the signal-to-noise ratio is high enough, and may be an important criterion for identification of subsurface alteration processes.
8. In the studied basalt powder spectra, both types of aridity, cold and hot, appear to be distinguishable from the contrasting spectral slope between 0.9 and 2.0 μm, at equivalent grain size. More data are required to determine whether this is a general feature that can be reliably used in the interpretation of spectra of the Martian surface.
9. The studied basalt samples display alteration products that reflect different alteration histories; nevertheless, from the combination of methods used, no criterion has been found that would help in identifying the origin of the weathering water–hydrothermal activity, groundwater, rainfall, or snowfall.

Although the alteration conditions of the two series of terrestrial basalt samples are contrasted, analysis of NIR spectra could not unequivocally discriminate between them. Other techniques are required for characterization of alteration differences that can accurately infer paleoclimate from altered basalts. Techniques aimed at identifying differences in kinetics of secondary mineral growth shall especially be investigated.

Part of the weathering of Icelandic basalts has been shown to have a biogenic origin (Etienne, 2002; Etienne and Dupont, 2002; Viles, 2008). Understanding the influence, if any, of the biological (fungi) communities on the NIR spectra of altered basalts is now a necessary step. If they do have any influence, comparison between spectral features on Earth and Mars may either be biased, or, if the

signature of fungi is diagnostic, reveal evidence for biogenic alteration of Martian basalts.

Acknowledgments

Field survey in Ogaden, sample collection and transport abroad were made possible by Pexco (East Africa) N.V., thanks to G. Tesfaye Gojji and B. Zewdie. Many thanks to M. Stelmaszczuk (Polish Academy of Sciences), A. Górski and T. Segit (University of Warsaw) for their help both in preparation of, and during the expedition to the Udokan volcanic field. Thanks are extended to G. Cornen (University of Nantes) for discussions on petrography of the studied samples, and R. Bonnefille (CEREGE) for expertize in Cenozoic climate evolution in Ethiopia. This study was funded by Région Pays de la Loire, France, through a postdoctoral grant awarded to J. Gurgurewicz, with additional contributions from National Planetology and Action Marges programmes of CNRS-INSU, Polish Ministry of Science and Higher Education/National Science Centre Grant no. N N307 065734, and Foundation for Polish Science Grant no. TEAM/2011-7/9.

Appendix A. Supplementary material

Supplementary data associated with this article can be found in the online version at http://dx.doi.org/10.1016/j.pss.2015.09.002.

References

Afonin, A.N., Greene, S.L., Dzyubenko, N.I., Frolov, A.N. (Eds.), 2008. Interactive Agricultural Ecological Atlas of Russia and Neighboring Countries. Economic Plants and their Diseases, Pests and Weeds [Online]. Available: ⟨http://www.agroatlas.ru⟩.

Anthony, J.W., Bideaux, R.A., Bladh, K.W., Nichols, M.C., 2003. Handbook of Mineralogy, vol. 2. Mineralogical Society of America, Chantilly, VA.

April, R.H., Keller, D.M., 1992. Saponite and vermiculite amygdales of the Granby basaltic tuff, Connecticut Valley. Clays Clay Miner. 40, 22–31.

Bandfield, J.L., Hamilton, V.E., Christensen, P.R., 2000. A global view of Martian surface compositions from MGS-TES. Science 287, 1626–1630.

Bell III, J.F., et al., 2004. Pancam multispectral imaging results from the Spirit rover at Gusev Crater. Science 305, 800–806. http://dx.doi.org/10.1126/science.1100175.

Bell III, J.F., Farrand, W.H., Johnson, J.R., Morris, R.V., 2002. Low abundance materials at the Mars pathfinder landing site: an investigation using spectral mixture analysis and related techniques. Icarus 158, 56–71. http://dx.doi.org/10.1006/icar.2002.6865.

Bender Koch, C., Mørup, S., Madsen, M.B., Vistisen, L., 1995. Iron-containing weathering products of basalt in a cold, dry climate. Chem. Geol. 122, 109–119.

Bibring, J.P., Langevin, Y., Mustard, J.F., Poulet, F., Arvidson, R., Gendrin, A., Gondet, B., Mangold, N., the OMEGA Team, 2006. Global mineralogical and aqueous Mars history derived from OMEGA/Mars express data. Science 312, 400–404. http://dx.doi.org/10.1126/science.1122659.

Bibring, J.P., Langevin, Y., Gendrin, A., Gondet, B., Poulet, F., Berthé, M., Soufflot, A., Arvidson, R., Mangold, N., Mustard, J., Drossart, P., The OMEGA Team, 2005. Mars surface diversity as revealed by the OMEGA/Mars express observations. Science 307, 1576–1581. http://dx.doi.org/10.1126/science.1108806.

Bishop, J.L., Pieters, C.M., Burns, R.G., 1993. Reflectance and Mössbauer spectroscopy of ferrihydrite montmorillonite assemblages as Mars soil analog materials. Geochim. Cosmochim. Acta 57, 4583–4595.

Bishop, J.L., Murchie, S.L., Pieters, C.M., Zent, A.P., 2002. A model for formation of dust, soil, and rock coatings on Mars: physical and chemical processes on the Martian surface. J. Geophys. Res. 107 (5097). http://dx.doi.org/10.1029/2001JE001581.

Bishop, J.L., Noe-Dobrea, Z., McKeown, N.K., Parente, M., Ehlmann, B.L., Michalski, J. R., Milliken, R.E., Poulet, F., Swayze, G.A., Mustard, J.F., Murchie, S.L., Bibring, J.P., 2008. Phyllosilicate diversity and past aqueous activity revealed at Mawrth Vallis, Mars. Science 321, 830–833. http://dx.doi.org/10.1126/science.1159699.

Bishop, J.L., Makarewicz, H.D., Gates, W.P., McKeown, N.K., Hiroi, T., 2010. Presence of beidellites on the Martian surface. In: Proceedings of the 21st Australian Clay Minerals Conference, Brisbane, Extended Abstracts, pp. 19–22.

Bobe, R., 2006. The evolution of arid ecosystems in eastern Africa. J. Arid Environ. 66, 564–584. http://dx.doi.org/10.1016/j.jaridenv.2006.01.010.

Bonnefille, R., 2010. Cenozoic vegetation, climate changes and hominid evolution in tropical Africa. Glob. Planet. Change 72, 390–412. http://dx.doi.org/10.1016/j.gloplacha.2010.01.015.

Bosellini, A., 1989. The continental margins of Somalia: their structural evolution and sequence stratigraphy. Mem. Sci. Geol. 41, 373–458.

Carr, M.H., Head III, J.W., 2010. Geologic history of Mars. Earth Planet. Sci. Lett. 294, 185–203. http://dx.doi.org/10.1016/j.epsl.2009.06.042.

Chevrier, V., Roy, R., Le Mouélic, S., Borschneck, D., Mathé, P.E., Rochette, P., 2006. Spectral characterization of weathering products of elemental iron in a Martian atmosphere: Implications for Mars hyperspectral studies. Planet. Space Sci. 54, 1034–1045. http://dx.doi.org/10.1016/j.pss.2005.12.019.

Chipera, S.J., Apps, J.A., 2001. Geochemical stability of natural zeolites. In: Bish, D.L., Ming, D. (Eds.), Natural Zeolites: Occurrence, Properties, Applications. Reviews in Mineralogy and Geochemistry, vol. 45, pp. 117–162.

Christensen, P.R., Bandfield, J.L., Smith, M.D., Hamilton, V.E., Clark, R.N., 2000. Identification of a basaltic component on the Martian surface from thermal emission spectrometer data. J. Geophys. Res. 105, 9609–9621.

Christensen, P.R., McSween Jr., H.Y., Bandfield, J.L., Ruff, S.W., Rogers, A.D., Hamilton, V.E., Gorelick, N., Wyatt, M.B., Jakosky, B.M., Kieffer, H.H., Malin, M.C., Moersch, J.E., 2005. Evidence for magmatic evolution and diversity on Mars from infrared observations. Nature 436, 504–509. http://dx.doi.org/10.1038/nature03639.

Clark, P.U., Alley, R.B., Pollard, D., 1999. Northern hemisphere ice-sheet influences on global climate change. Science 286, 1104–1111.

Clark, R.N., Roush, T.L., 1984. Reflectance spectroscopy: quantitative analysis techniques for remote sensing applications. J. Geophys. Res. 89, 6329–6340.

Clark, R.N., King, T.V.V., Klejwa, M., Swayze, G.A., 1990. High spectral resolution reflectance spectroscopy of minerals. J. Geophys. Res. 95, 12653–12680.

Clark, R.N., Swayze, G.A., Wise, R., Livo, E., Hoefen, T., Kokaly, R., Sutley, S.J., 2007. USGS digital spectral library splib06a. Digital Data Series 231. U.S. Geological Survey, Denver, ⟨http://speclab.cr.usgs.gov/spectral.lib06⟩.

Cloutis, E.A., 1992. Weathered and unweathered surface spectra of rocks from cold deserts: identification of weathering processes and remote sensing implications. Geol. Fören. Stockh. Förh. 114, 181–191.

Cloutis, E.A., Grasby, S.E., Last, W.M., Léveillé, R., Osinski, G.R., Sherriff, B.L., 2010. Spectral reflectance properties of carbonates from terrestrial analogue environments: implications for Mars. Planet. Space Sci. 58, 522–537. http://dx.doi.org/10.1016/j.pss.2009.09.002.

Cloutis, E.A., 2004. Spectral reflectance properties of some basaltic weathering products. In: Proceedings of the 35th Lunar and Planetary Science Conference, Houston, Texas, Paper 1265.

Cole, D.R., Ravinsky, L.I., 1984. Hydrothermal alteration zoning in the Beowave geothermal system, Eureka and Lander counties, Nevada. Econ. Geol. 79, 759–767.

Curran, P.J., 1989. Remote sensing of foliar chemistry. Remote Sens. Environ. 30, 271–278.

Deepthy, R., Balakrishnan, S., 2005. Climatic control on clay mineral formation: evidence from weathering profiles developed on either side of the Western Ghats. J. Earth Syst. Sci. 114, 545–556. http://dx.doi.org/10.1007/BF02702030.

deMenocal, P., 1995. Plio-Pleistocene African climate. Science 270, 53–59.

Demske, D., Heumann, G., Granoszewski, W., Nita, M., Mamakowa, K., Tarasov, P.E., Oberhänsli, H., 2005. Late glacial and Holocene vegetation and regional climate variability evidenced in high-resolution pollen records from Lake Baikal. Glob. Planet. Change 46, 255–279.

Edwards, C.S., Christensen, P.R., Hamilton, V.E., 2008. Evidence for extensive olivine-rich basalt bedrock outcrops in Ganges and Eos chasmas, Mars. J. Geophys. Res. 113, E11003. http://dx.doi.org/10.1029/2008JE003091.

Ehlmann, B.L., Mustard, J.F., Swayze, G.A., Clark, R.N., Bishop, J.L., Poulet, F., Des Marais, D.J., Roach, L.H., Milliken, R.E., Wray, J.J., Barnouin-Jha, O., Murchie, S.L., 2009. Identification of hydrated silicate minerals on Mars using MRO-CRISM: geologic context near Nili Fossae and implications for aqueous alteration. J. Geophys. Res. 114, E00D08. http://dx.doi.org/10.1029/2009JE003339.

Ehlmann, B.L., Mustard, J.F., Murchie, S.L., Poulet, F., Bishop, J.L., Brown, A.J., Calvin, W.M., Clark, R.N., Des Marais, D.J., Milliken, R.E., Roach, L.H., Roush, T.L., Swayze, G.A., Wray, J.J., 2008. Orbital identification of carbonate-bearing rocks on Mars. Science 322, 1828–1832. http://dx.doi.org/10.1126/science.1164759.

Elvidge, C.D., 1990. Visible and near infrared reflectance characteristics of dry plant materials. Int. J. Remote Sens. 11, 1775–1795.

Enikeev, F.I., 2008. The late Cenozoic of northern Transbaikalia and paleoclimates of southern East Siberia. Russ. Geol. Geophys. 49, 602–610.

Etienne, S., 2002. The role of biological weathering in periglacial areas: a study of weathering rinds in south Iceland. Geomorphology 47, 75–86.

Etienne, S., Dupont, J., 2002. Fungal weathering of basaltic rocks in a cold oceanic environment (Iceland): comparison between experimental and field observations. Earth Surf. Process. Landf. 27, 737–748. http://dx.doi.org/10.1002/esp.349.

Feakins, S.J., 2013. Pollen-corrected leaf wax D/H reconstructions of northeast African hydrological changes during the late Miocene. Palaeogeogr. Palaeoclimatol. Palaeoecol. 374, 62–71. http://dx.doi.org/10.1016/j.palaeo.2013.01.004.

Feakins, S.J., deMenocal, P.B., Eglington, T.I., 2005. Biomarker records of late Neogene changes in northeast African vegetation. Geology 33, 977–980. http://dx.doi.org/10.1130/G21814.1.

Gaffey, S.J., 1986. Spectral reflectance of carbonate minerals in the visible and near infrared (0.35–2.55 microns): calcite, aragonite, and dolomite. Am. Mineral. 71, 151–162.

Gaudin, A., Dehouck, E., Mangold, N., 2011. Evidence for weathering on early Mars from a comparison with terrestrial weathering profiles. Icarus 216, 257–268. http://dx.doi.org/10.1016/j.icarus.2011.09.004.

Glotch, T.D., Rogers, A.D., 2013. Evidence for magma–carbonate interaction beneath Syrtis Major, Mars. J. Geophys. Res. 118, 126–137. http://dx.doi.org/10.1029/2012JE004230.

Grygar, T., Bezdicka, P., Hradil, D., Hruskova, M., Novotna, K., Kadlec, J., Pruner, P., Oberhansli, H., 2005. Characterization of expandable clay minerals in lake Baikal sediments by thermal dehydration and cation exchange. Clays Clay Miner. 53, 389–400. http://dx.doi.org/10.1346/CCMN.2005.0530407.

Gurgurewicz, J., 2010. Alteration of Martian Basalts and Implications for the Evolution of Martian Climate: Study of Terrestrial Analogs. University of Nantes/Pays de la Loire Region, Nantes, France, p. 56.

Hamilton, V.E., Wyatt, M.B., McSween Jr., H.Y., Christensen, P.R., 2001. Analysis of terrestrial and Martian volcanic compositions using thermal emission spectroscopy: 2. Application to Martian surface spectra from the Mars Global Surveyor Thermal Emission Spectrometer. J. Geophys. Res. 106, 14733–14746.

Hapke, B.W., 1993. Theory of Reflectance and Emittance Spectroscopy. Cambridge University Press, New York, p. 455.

Harloff, J., Arnold, G., 2001. Near-infrared reflectance spectroscopy of bulk analog materials for planetary crust. Planet. Space Sci. 49, 191–211.

Hiroi, T., Pieters, C.M., 1994. Estimation of grain sizes and mixing ratios of fine powder mixtures of common geologic minerals. J. Geophys. Res. 99, 10867–10879.

Huang, Y., Clemens, S.C., Liu, W., Wang, Y., Prell, W.L., 2007. Large-scale hydrological change drove the late Miocene C_4 plant expansion in the Himalayan foreland and Arabian Peninsula. Geology 35, 531–534.

Hunt, G.R., 1977. Spectral signature of particulate minerals in the visible and near infrared. Geophysics 42, 501–513.

Hunt, G.R., Salisbury, J.W., Lenhoff, C.J., 1974. Visible and near infrared spectra of minerals and rocks: IX. Basic and ultrabasic igneous rocks. Mod. Geol. 5, 15–22.

Hynek, B.M., McCollom, T.M., Marcucci, E.C., Brugman, K., Rogers, K.L., 2013. Assessment of environmental controls on acid-sulfate alteration at active volcanoes in Nicaragua: applications to relic hydrothermal systems on Mars. J. Geophys. Res. Planets 118, 2083–2104. http://dx.doi.org/10.1002/jgre.20140.3.

International Centre for Diffraction Data (ICDD) [Online]. Available: ⟨http://www.icdd.com⟩.

Izawa, M.R.M., Applin, D.M., Norman, L., Cloutis, E.A., 2014. Reflectance spectroscopy (350–2500 nm) of solid-state polycyclic aromatic hydrocarbons (PAHs). Icarus 237, 159–181. http://dx.doi.org/10.1016/j.icarus.2014.04.033.

Jacobs, B.F., 2004. Palaeobotanical studies from tropical Africa: relevance to the evolution of forest, woodland and savannah biomes. Philos. Trans. R. Soc. Lond. B 359, 1573–1583. http://dx.doi.org/10.1098/rstb.2004.1533.

Jacobs, B.F., Tabor, N., Feseha, M., Pan, A., Kappelman, J., Rasmussen, T., Sanders, W., Wiemann, M., Crabaugh, J., Massini, J.L. Garcia, 2005. Oligocene terrestrial strata of northwestern Ethiopia: a preliminary report on paleoenvironments and paleontology. Palaeontol. Electron. 8, 1.25A.

Köhler, B., Singer, A., Stoffers, P., 1994. Biogenic nontronite from marine white smoker chimneys. Clays Clay Miner. 42, 689–701.

Kanner, L.C., Mustard, J.F., Gendrin, A., 2007. Assessing the limits of the Modified Gaussian Model for remote spectroscopic studies of pyroxenes on Mars. Icarus 187, 442–456. http://dx.doi.org/10.1016/j.icarus.2006.10.025.

Koeppen, W.C., Hamilton, V.E., 2008. Global distribution, composition, and abundance of olivine on the surface of Mars from thermal infrared data. J. Geophys. Res. 113, E05001. http://dx.doi.org/10.1029/2007JE002984.

Kohler, T., Krauer, J., 1996. Ethio-GIS und Agro-ökologische Karte Äthiopien. Landesbericht der Schweizerischen Gesellschaft für Kartographie. 13. Kartographische Publikationsreihe, Switzerland, pp. 34–38.

Kuebler, K.E., 2013. A comparison of the iddingsite alteration products in two terrestrial basalts and the Allan Hills 77005 Martian meteorite using Raman spectroscopy and electron microprobe analyses. J. Geophys. Res. 118, 803–830. http://dx.doi.org/10.1029/2012JE004243.

Le Deit, L., Flahaut, J., Quantin, C., Hauber, E., Mège, D., Bourgeois, O., Gurgurewicz, J., Massé, M., Jaumann, R., 2012. Extensive surface pedogenic alteration of the Martian Noachian crust suggested by plateau phyllosilicates around Valles Marineris. J. Geophys. Res. 117, E00J05. http://dx.doi.org/10.1029/2011JE003983.

Levrard, B., Forget, F., Montmessin, F., Laskar, J., 2004. Recent ice-rich deposits formed at high latitudes on Mars by sublimation of unstable equatorial ice during low obliquity. Nature 1072–1075 (431). http://dx.doi.org/10.1038/nature03055.

Long, D.A., 2002. The Raman Effect: A Unified Treatment of the Theory of Raman Scattering by Molecules. John Wiley & Sons Ltd., Chichester, United Kingdom, p. 598.

Lysak, S., 1995. Terrestrial heat and temperatures in the upper crust in South East Siberia. Bull. Centres Rech. Explor. Prod. ELF Aquitaine 19, 39–57.

Mège, D., Masson, P., 1996. A plume tectonics model for the Tharsis province, Mars. Planet. Space Sci. 44 (12), 1499–1546.

Mège, D., Korme, T., 2004. Dyke swarm emplacement in the Ethiopian Large Igneous Province: not only a matter of stress. J. Volcanol. Geotherm. Res. 132, 283–310.

Mège, D., Purcell, P., Pochat, S., Guidat, T., 2015a. The landscape and landforms of the Ogaden, Southeast Ethiopia. In: Billi, P. (Ed.), Landscapes and Landforms of Ethiopia. Springer, pp. 323–348. http://dx.doi.org/10.1007/978-94-017-8026-1_19.

Mège, D., Cook, A.C., Lagabrielle, Y., Garel, E., Cormier, M.H., 2003. Volcanic rifting at Martian grabens. J. Geophys. Res. 108. http://dx.doi.org/10.1029/2002JE001852.

Mège, D., Purcell, P.G., Bézos, A., Jourdan, F., La, C., 2015b. A major dyke swarm in the Ogaden region south of Afar and the early evolution of the Afar Triple Junction. In: Wright, T.J., Ayele, A., Ferguson, D.J., Kidane, T., Vye-Brown, C. (Eds.), Magmatic Rifting and Active Volcanism, Geological Society, Special Publications, London, 420, http://dx.doi.org/10.1144/SP420.7.

Mège, D., Gaudin, A., Morizet, Y., 2008. Geology of Ogaden blocks 18-19-21, Ethiopia (Pexco concession), observations and preliminary results. In: Proceedings of the Pexco Exploration (East Africa) N.V., Kuala Lumpur, p. 66.

Mège, D., Purcell, P., 2010. Ethiopian flood basalt province: 2. The Ogaden Dyke Swarm. In: Proceedings of the 6th International Dyke Conference, Varanasi, India, Paper 84.

Malyshev, L.L., Latrix Dahurica. In: Afonin, A.N., Greene, S.L., Dzyubenko, N.I., Frolov, A.N. (Eds.), 2008. Interactive Agricultural Ecological Atlas of Russia and Neighboring Countries. Economic Plants and their Diseases, Pests and Weeds [Online]. Available: ⟨http://www.agroatlas.ru/en/content/related/Larix_dahurica⟩.

McEwen, A.S., Malin, M.C., Carr, M.H., Hartmann, W.K., 1999. Voluminous volcanism in early Mars revealed in Valles Marineris. Nature 397, 584–586.

McKeown, N.K., Bishop, J.L., Noe Dobrea, E.Z., Ehlmann, B.L., Parente, M., Mustard, J. F., Murchie, S.L., Swayze, G.A., Bibring, J.P., Silver, E.A., 2009. Characterization of phyllosilicates observed in the central Mawrth Vallis region, Mars, their potential formational processes, and implications for past climate. J. Geophys. Res. 114, E00D10. http://dx.doi.org/10.1029/2008JE003301.

McSween, H.Y., et al., 2004. Basaltic rocks analyzed by the Spirit rover in Gusev crater. Science 305, 842–845.

Micheels, A., Eronen, J., Mosbrugger, V., 2009. The Late Miocene climate response to a modern Sahara desert. Global Planet. Change 67, 193–204. http://dx.doi.org/10.1016/j.gloplacha.2009.02.005.

Miller, C.E., 2001. Chemical principles of near-infrared technology. In: Williams, P. H., Norris, K. (Eds.), Near-Infrared Technology In The Agricultural and Food Industries, second edition AACC, St. Paul, MN, USA, pp. 19–37.

Moore, D.M., Reynolds Jr., R.C., 1997. X-Ray Diffraction and the Indentification and Analysis of Clay Minerals. Oxford University Press, Oxford, New York, p. 378.

Morizet, Y., Paris, M., Gaillard, F., Scaillet, B., 2010. C–O–H fluid solubility in haplobasalt under reducing conditions: an experimental study. Chem. Geol. 279, 1–16. http://dx.doi.org/10.1016/j.chemgeo.2010.09.011.

Morris, R.V., Neely, S.C., Mendell, W.W., 1982. Application of Kubelka–Munk theory of diffuse reflectance to geologic problems: the role of scattering. Geophys. Res. Lett. 9, 113–116.

Morris, R.V., Golden, D.C., Bell III, J.F., 1997. Low-temperature reflectivity spectra of red hematite and the color of Mars. J. Geophys. Res. 102, 9125–9133.

Morris, R.V., Ruff, S.W., Gellert, R., Ming, D.W., Arvidson, R.E., Clark, B.C., Golden, D. C., Siebach, K., Klingelhöfer, G., Schröder, C., Fleischer, I., Yen, A.S., Squyres, S.W., 2010. Identification of carbonate-rich outcrops on Mars by the Spirit rover. Science 329, 421–424. http://dx.doi.org/10.1126/science.1189667.

Morris, R.V., Klingelhöfer, G., Bernhardt, B., Schröder, C., Rodionov, D.S., de Souza Jr., P.A., Yen, A., Gellert, R., Evlanov, E.N., Foh, J., Kankeleit, E., Gütlich, P., Ming, D. W., Renz, F., Wdowiak, T., Squyres, S.W., Arvidson, R.E., 2004. Mineralogy at Gusev Crater from the Mössbauer Spectrometer on the Spirit Rover. Science 305, 833–836. http://dx.doi.org/10.1126/science.1100020.

Mustard, J.F., et al., 2008. Hydrated silicate minerals on Mars observed by the Mars Reconnaissance Orbiter CRISM instrument. Nature 454, 305–309. http://dx.doi.org/10.1038/nature07097.

Mustard, J.F., Poulet, F., Gendrin, A., Bibring, J.P., Langevin, Y., Gondet, B., Mangold, N., Bellucci, G., Altieri, F., 2005. Olivine and pyroxene diversity in the crust of Mars. Science 307, 1594–1597. http://dx.doi.org/10.1126/science.1109098.

Neuville, D.R., Mysen, B.O., 1996. Role of the Al in the silicate network: in situ, high temperature study of glasses and melts on the join SiO_2–$NaAlO_2$. Geochim. Cosmochim. Acta 60, 1727–1737.

NOAA Climate Prediction Center, 2012. [Online]. Available: ⟨http://www.cpc.noaa.gov/products/fews/AFR_CLIM/afr_clim.htmlseasonal_archived⟩ (Consulted in August 2012).

Nyquist, L.E., Bogard, D.D., Shih, C.Y., Greshake, A., Stöffler, D., Eugster, O., 2001. Ages and geologic histories of Martian meteorites. Space Sci. Rev. 96, 105–164.

PDS Geosciences Spectral Library Service [Online]. Available: ⟨http://speclib.rsl.wustl.edu⟩.

Peel, F.C., Finlayson, B.L., McMahon, T.A., 2007. Updated world map of the Köppen–Geiger classification. Hydrol. Earth Syst. Sci. 11, 1633–1644.

Petit, C., Déverchère, J., 2006. Structure and evolution of the Baikal rift: a synthesis. Geochem. Geophys. Geosyst. 7, Q11016. http://dx.doi.org/10.1029/2006GC001265.

Poulet, F., Gomez, C., Bibring, J.P., Langevin, Y., Gondet, B., Pinet, P., Belluci, G., Mustard, J., 2007. Martian surface mineralogy from Observatoire pour la Mine ´ralogie, l'Eau, les Glaces et l'Activite´ on board the Mars Express spacecraft (OMEGA/MEx): global mineral maps. J. Geophys. Res. 112, E08S02. http://dx.doi.org/10.1029/2006JE002840.

Poulet, F., Bibring, J.P., Mustard, J.F., Gendrin, A., Mangold, N., Langevin, Y., Arvidson, R.E., Gondet, B., Gomez, C., the Omega Team, 2005. Phyllosilicates on Mars and implications for early Martian climate. Nature 438, 623–627. http://dx.doi.org/10.1038/nature04274.

Poulet, F., Bibring, J.P., Langevin, Y., Mustard, J.F., Mangold, N., Vincendon, M., Gondet, B., Pinet, P., Bardintzeff, J.-M., Platevoët, B., 2009. Quantitative compositional analysis of Martian mafic regions using the MEx/OMEGA reflectance data: 1. Methodology, uncertainties and examples of application. Icarus 201, 69–83. http://dx.doi.org/10.1016/j.icarus.2008.12.025.

Pound, M.J., Haywood, A.M., Salzmann, U., Riding, J.B., 2012. Global vegetation dynamics and latitudinal temperature gradients during the Mid to Late

Miocene (15.97–5.33 Ma). Earth-Sci. Rev. 112, 1–22. http://dx.doi.org/10.1016/j.earscirev.2012.02.005.
Rasskazov, S.V., 1994. Magmatism related to the Eastern Siberia rift system and the geodynamics. Bull. Centres Rech. Explor.-Prod. Elf Aquitaine 18, 437–452.
Roach, L.H., Mustard, J.F., Swayze, G., Milliken, R.E., Bishop, J.L., Murchie, S.L., Lichtenberg, K., 2010. Hydrated mineral stratigraphy in Ius Chasma, Valles Marineris. Icarus 206, 253–268. http://dx.doi.org/10.1016/j.icarus.2009.09.003.
Rogers, A.D., Christensen, P.R., 2007. Surface mineralogy of Martian low-albedo regions from MGS-TES data: implications for upper crustal evolution and surface alteration. J. Geophys. Res. 112, E01003. http://dx.doi.org/10.1029/2006JE002727.
Rogers, A.D., Aharonson, O., 2008. Mineralogical composition of sands in Meridiani Planum determined from Mars Exploration Rover data and comparison to orbital measurements. J. Geophys. Res. 113, E06S14. http://dx.doi.org/10.1029/2007JE002995.
Rogers, A.D., Bandfield, J.L., Christensen, P.R., 2007. Global spectral classification of Martian low albedo regions with Mars Global Surveyor Thermal Emission Spectrometer (MGS-TES) data. J. Geophys. Res. 112, E02004. http://dx.doi.org/10.1029/2006JE002726.
Salvatore, M.R., Mustard, J.F., Wyatt, M.B., Murchie, S.L., 2010. Definitive evidence of Hesperian basalt in Acidalia and Chryse planitiae. J. Geophys. Res. 115, E07005. http://dx.doi.org/10.1029/2009JE003519.
Sepulchre, P., Ramstein, G., Fluteau, F., Schuster, M., Tiercelin, J.J., Brunet, M., 2006. Tectonic uplift and eastern Africa aridification. Science 313, 1419–1423.
Shchetnikov, A.A., White, D., Filinov, I.A., Rutter, N., 2012. Late Quaternary geology of the Tunka rift basin (Lake Baikal region), Russia. J. Asian Earth Sci. 46, 195–208.
Sheinkman, V., 2003. Quaternary glaciation and its influence on environment in the high mountains of central Siberia. Geol. Soc. Am. Abst. Programs 169 (Paper 54-2).
SRK Consulting, 2010. Udokan Project Environmental and Socials Coping Study. Scoping Rep. RU0229. Baikal Mining Company, Udokan, Russia.
SRK Consulting, 2014. Non-technical Summary of Report on the Detailed Environmental Impact Assessment for the Udokan Project. Baikal Mining Company, Udokan, Russia, p. 111.
Stupak, F.M., Lebedev, V.A., Kudryashova, E.A., 2008. The stages and distribution areas of the Late Cenozoic volcanism in the Udokan Range in Transbaikalia based on geochronologic studies. J. Volcanol. Seismol. 2, 30–39.
Swindle, T.D., Treiman, A.H., Lindstrom, D.J., Burkland, M.K., Cohen, B.A., Grier, J.A., Li, B., Olson, E.K., 2000. Noble gases in iddingsite from the Lafayette meteorite: evidence for liquid water on Mars in the last few hundred million years. Meteorit. Planet. Sci. 35, 107–115.
Tarasov, P.E., Bezrukova, E.V., Krivonogov, S.K., 2009. Late Glacial and Holocene changes in vegetation cover and in climate in southern Siberia derived from a 15 kyz long pollen record from Lake Kotokel. Clim. Past 5, 285–295.
Tchebakova, N.M., Rehfeldt, G.E., Parfenova, E.I., 2005. Impacts of climate change on the distribution of *Larix* spp. and *Pinus sylvestris* and their climatypes in Siberia. Mitig. Adapt. Strateg. Glob. Change 11, 861–882. http://dx.doi.org/10./1007/s11027-005-9019-0.
Treiman, A.H., Lindstrom, D.J., 1997. Trace element geochemistry of Martian iddingsite in the Lafayette meteorite. J. Geophys. Res. 102, 9153–9163.
Treiman, A.H., Barrett, R.A., Gooding, J.L., 1993. Preterrestrial aqueous alteration of the Lafayette (SNC) meteorite. Meteoritics 28, 86–97.
Viles, H.A., 2008. Understanding dryland landscape dynamics: do biological crusts hold the key? Geogr. Compass 2–3, 899–919. http://dx.doi.org/10.1111/j.1749-8198.2008.00099.x.
Vogt, T., Larqué, P., 2002. Clays and secondary minerals as permafrost indicators: examples from the circum-Baikal region. Quart. Int. 95–96, 175–187.
Vogt, T., Clauer, N., Larqué, P., 2010. Impact of climate and related weathering processes on the authigenesis of clay minerals: examples from circum-Baikal region, Siberia. Catena 80, 53–64. http://dx.doi.org/10.1016/j.catena.2009.08.008.
Winkler, A.J., 2002. Neogene paleobiogeography and East African paleoenvironments: contributions from the Tugen Hills rodents and lagomorphs. J. Hum. Evol. 42, 237–256. http://dx.doi.org/10.1006/jhev.2001.0501.
Wyatt, M.B., McSween Jr., H.Y., 2002. Spectral evidence for weathered basalt as an alternative to andesite in the northern lowlands of Mars. Nature 417, 263–266.
Wyatt, M.B., Hamilton, V.E., McSween Jr., H.Y., Christensen, P.R., Taylor, L.A., 2001. Analysis of terrestrial and Martian volcanic using thermal emission spectroscopy: 1. Determination of mineralogy, chemistry, and classification strategies. J. Geophys. Res. 106, 14711–14732.